arXiv:2311.08490v2 [hep-ex] 4 Sep 2024

Observation of strangeness enhancement with charmed mesons in high-multiplicity pPb collisions at $\sqrt{s_{\mathrm{NN}}} = 8.16$ TeV

LHCb collaboration[†]

Abstract

The production of prompt D_s^+ and D^+ mesons is measured by the LHCb experiment in proton-lead (pPb) collisions in both the forward ($1.5 < y^* < 4.0$) and backward ($-5.0 < y^* < -2.5$) rapidity regions at a nucleon-nucleon center-of-mass energy of $\sqrt{s_{\mathrm{NN}}} = 8.16$ TeV. The nuclear modification factors of both D_s^+ and D^+ mesons are determined as a function of transverse momentum, p_{T}, and rapidity. In addition, the D_s^+ to D^+ cross-section ratio is measured as a function of the primary charged particle multiplicity in the event. An enhanced D_s^+ to D^+ production in high-multiplicity events is observed for the whole measured p_{T} range, in particular at low p_{T} and backward rapidity, where the significance exceeds six standard deviations. This constitutes the first observation of strangeness enhancement in charm quark hadronization in high-multiplicity pPb collisions. The results are also qualitatively consistent with the presence of quark coalescence as an additional charm quark hadronization mechanism in high-multiplicity proton-lead collisions.

[†]Authors are listed at the end of this paper.

At hadron colliders, charm quarks are mainly produced by hard parton-parton interactions in the initial stages of the collisions, which are well described by perturbative quantum chromodynamics (pQCD) calculations. These calculations are based on the factorisation theorem, according to which the charmed hadron cross-sections are dependent on the parton distribution functions (PDFs) of the incoming nucleons, the hard parton-parton scattering cross-section, and the fragmentation functions [1, 2].

In proton–lead collisions, various effects could modify the charmed hadron cross-sections compared to pp collisions. In the initial state, the charmed hadron production can be affected by the modification of the parton distribution functions of bound nucleons (nPDFs) [3, 4] compared to those of free nucleons. Furthermore, the increased gluon density at small momentum fraction x leads to non-perturbative features, even if the coupling constant is weak. The color-glass condensate (CGC) effective theory [5, 6] provides an appropriate theoretical framework in this regime. A recent measurement from the LHCb experiment has shown a discrepancy with the theoretical calculations based on nPDFs [7]. In the final state, the fragmentation functions are typically parameterised based on measurements performed in e^+e^- or ep collisions, assuming that the hadronization of charm quarks to charmed hadrons is a universal process independent of the colliding system [8]. A recent measurement from the ALICE experiment has shown that charm quark hadronization differs between e^+e^- and pp collisions [9, 10]. This result suggests the existence of other hadronization mechanisms beyond fragmentation. An alternative mechanism is quark coalescence [11–14], where charm quarks recombine with other quarks to form charmed hadrons. This mechanism requires that multiple quarks overlap in velocity-position space. As a result, the fraction of charmed hadrons produced by coalescence is expected to be larger when the number of quarks produced in the collision is large, for example in relativistic heavy-ion collisions where quark-gluon plasma (QGP) is formed [15, 16]. This mechanism is also expected to be more prominent at relatively low transverse momentum, p_{T}, as most quarks or particles are produced in that kinematic region.

Relativistic heavy-ion collisions are often accompanied by strangeness enhancement, which was originally considered as a signature of QGP [17]. The enhanced strangeness production [18, 19] and the coalescence mechanism result in an increased yield of strange charmed mesons relative to non-strange charmed mesons compared to pp collisions [20, 21]. Additionally, the ALICE collaboration observed the production enhancement of strange light hadrons in both high-multiplicity pp [22] and pPb [23, 24] collisions. Although the origin of the strangeness enhancement in "small" systems (proton-proton or proton-nucleus collisions) is still under debate [25, 26], it may indicate a common underlying physics mechanism which gradually compensates the strangeness suppression in fragmentation. If the coalescence mechanism contributes to the charm quark hadronization in small systems, the production rates of D_s^+ mesons ($c\bar{s}$) relative to D^+ mesons ($c\bar{d}$) could also increase with the event multiplicity.

This letter reports LHCb measurements of the prompt $D_{(s)}^+$ (D_s^+ and D^+) differential production cross-sections, of their nuclear modification factors and forward-backward cross-section ratio in pPb collisions at $\sqrt{s_{\mathrm{NN}}} = 8.16$ TeV. Additionally, the cross-section ratio, $\sigma_{D_s^+}/\sigma_{D^+}$, as a function of the primary charged particle multiplicity of the events is reported.

The LHCb detector is a single-arm forward spectrometer covering the pseudorapidity range $2 < \eta < 5$, described in detail in Refs. [27, 28]. The present measurement covers the

forward rapidity range of $1.5 < y^* < 4.0$ when the proton beam points towards the LHCb arm, and the backward rapidity range of $-5.0 < y^* < -2.5$ when the lead beam does. Here, y^* is the rapidity in the nucleon-nucleon center-of-mass frame. The centre-of-mass frame does not coincide with the laboratory frame due to the asymmetry of the colliding beam energies, with a constant boost of $y_{\mathbf{lab}} - y^* = 0.5 \log(A/Z) = 0.465$ in the direction of the proton beam, where $A = 208$ is the lead nucleus mass number and $Z = 82$ is the lead nucleus atomic number. The corresponding integrated luminosity for the forward (backward) rapidity data sample is $12.18 \pm 0.32\,\mathrm{nb}^{-1}$ ($18.57 \pm 0.46\,\mathrm{nb}^{-1}$).

Simulation is used to model the effects of detector acceptance and selection requirements. The $D^+_{(s)}$ mesons are generated using Pythia 8 [29] and embedded into minimum-bias (MB) pPb events using the EPOS generator [30], calibrated with LHC data [31]. The decays of unstable particles are described by EvtGen [32], in which final-state radiation is generated using PHOTOS [33]. The interaction of the generated particles with the detector, and its response, are implemented using the Geant4 toolkit [34] as described in Ref. [35]. The simulated $D^+_{(s)}$ event multiplicity distribution is weighted to match the background-subtracted distribution that is extracted from data using the *sPlot* method [36].

The double-differential cross-section in a given (p_{T}, y^*) interval is defined as

$$\frac{\mathrm{d}^2\sigma_{p\mathrm{Pb}}}{\mathrm{d}p_{\mathrm{T}}\mathrm{d}y^*} = \frac{N}{\mathcal{L} \times \epsilon^{\mathrm{acc}} \times \epsilon^{\mathrm{trig}} \times \epsilon^{\mathrm{PID}} \times \epsilon^{\mathrm{rec\&sel}} \times \mathcal{B} \times \Delta p_{\mathrm{T}} \times \Delta y^*} \ , \tag{1}$$

where N is the observed number of prompt $D^+_{(s)}$ and $D^-_{(s)}$ mesons, $\mathcal{L}$ the integrated luminosity, $\mathcal{B}$ the branching fraction of the corresponding $D^+_{(s)}$ meson decay, ϵ^{acc}, ϵ^{trig}, ϵ^{PID}, $\epsilon^{\mathrm{rec\&sel}}$ are the LHCb acceptance, trigger, particle identification (PID), reconstruction and selection efficiencies, respectively, and Δp_{T} and Δy^* are the p_{T} and y^* interval widths. The $D^+_{(s)}$ mesons are reconstructed through the $D^+ \to K^-\pi^+\pi^+$ and $D^+_s \to K^-K^+\pi^+$ decay channels, where the mass of the K^+K^- pair is required to be within $20\,\mathrm{MeV}/c^2$ of the known mass of the $\phi(1020)$ meson. The corresponding branching fractions are $\mathcal{B} = (2.24 \pm 0.13)\%$ for the $D^+_s \to K^-K^+\pi^+$ decay [37], and $\mathcal{B} = (9.38 \pm 0.16\%)$ for the $D^+ \to K^-\pi^+\pi^+$ decay [38].

The selection criteria applied to $D^+_{(s)}$ candidates are similar to those used in the recent D^0 production measurements in pPb collisions at $\sqrt{s_{\mathrm{NN}}} = 8.16$ TeV [7].

The sample of $D^+_{(s)}$ candidates includes $D^+_{(s)}$ mesons originating from the collision point and from the decay of b hadrons. These categories are referred to as "prompt" and "from-b", respectively. The inclusive signal yield is determined using an extended unbinned maximum-likelihood fit to the invariant-mass distributions of the $K^-K^+\pi^+$ or $K^-\pi^+\pi^+$ combinations. The invariant mass of the signal is described by the sum of a Crystal Ball function [39] and a Gaussian function, where both functions share a common mean, while the background shape is described by a linear function. The prompt signal yield is determined by fitting the distribution of $\log_{10}(\chi^2_{\mathrm{IP}})$ of the candidates, where χ^2_{IP} is defined as the difference in the vertex-fit χ^2 of a given primary vertex (PV) reconstructed with and without the candidate under consideration. Combinatorial background in the $\log_{10}(\chi^2_{\mathrm{IP}})$ distribution is subtracted using the *sPlot* method with the charm meson invariant mass as discriminating variable. The shapes of the $\log_{10}(\chi^2_{\mathrm{IP}})$ distributions corresponding to the prompt and from-b components are described by Bukin functions [40]. The parameters of the function describing the from-b component are fixed from simulation, and the parameters describing the prompt component are allowed to float. Typical invariant mass

and $\log_{10}(\chi^2_{\mathrm{IP}})$ distributions are shown in the Supplemental Material [41].

The LHCb acceptance, trigger, reconstruction and selection efficiencies are evaluated with pPb simulated samples. The track reconstruction efficiency is calibrated with MB $J/\psi \to \mu^+\mu^-$ and $K^0_S \to \pi^+\pi^-$ samples, using the tag-and-probe approach of Ref. [42]. The PID efficiencies are estimated using a tag-and-probe method [43, 44].

The various sources of systematic uncertainties considered in this measurement are listed in Table 1. The uncertainty from the invariant mass fit is determined by describing signal and background shapes with alternative models [45]. For the estimation of the uncertainty associated to the $\log_{10}(\chi^2_{\mathrm{IP}})$ fit, the data are fitted again with different models and after varying any fixed parameters to evaluate the change in signal yield. The uncertainties on the tracking and PID calibration are dominated by the limited size of calibration samples. The uncertainty associated to the simulation multiplicity correction is estimated by weighting simulated events using different multiplicity variables. The larger uncertainty from multiplicity corrections in the backward region primarily stems from a worse agreement between simulation and data in that region. For the trigger efficiency, the difference between the efficiencies derived from simulation and from collision data [46] are considered as a systematic uncertainty. The uncertainties associated to the luminosity, the branching fractions and the simulated samples size are also included.

Table 1: Systematic uncertainties on the measured double-differential cross-section. Each range indicates the minimum and the maximum value across all kinematic intervals. The uncertainties due to the mass and $\log_{10}(\chi^2_{\mathrm{IP}})$ fits are uncorrelated across the intervals. The other sources of uncertainty are 100% correlated between the different intervals.

Uncertainty source	Forward [%]	Backward [%]
Mass fit	$0.1 - 6.1$	$0.1 - 9.6$
$\log_{10}(\chi^2_{\mathrm{IP}})$ fit	$0.1 - 22.2$	$0.1 - 17.3$
Tracking calibration	$0.9 - 3.6$	$1.4 - 9.6$
PID calibration	$1.2 - 14.0$	$1.4 - 8.9$
Multiplicity correction	$0.5 - 3.5$	$4.9 - 11.3$
Trigger efficiency	$0.0 - 1.6$	$0.0 - 1.5$
Luminosity	2.6	2.5
Branching fraction D_s^+	5.8	5.8
Branching fraction D^+	1.7	1.7

The double-differential cross-sections for prompt D_s^+ (D^+) mesons are measured in the p_{T} range $1 < p_{\mathrm{T}} < 13$ GeV/c ($1 < p_{\mathrm{T}} < 14$ GeV/c) and the rapidity ranges $1.5 < y^* < 4.0$ and $-5.0 < y^* < -2.5$ for the forward and backward rapidity regions, respectively. The results and numerical values are given in the Supplemental Material [41]. The total prompt $D_{(s)}^+$ production cross-sections, obtained by integrating the double-differential results in the measured kinematic ranges, are $42.83 \pm 0.29 \pm 3.45$ mb ($92.36 \pm 0.18 \pm 4.96$ mb) for the forward rapidity region, and $42.96 \pm 0.36 \pm 4.91$ mb ($84.09 \pm 0.17 \pm 8.39$ mb) for the backward rapidity region, where the first uncertainty is statistical and the second systematic.

The nuclear modification factor $R_{p\mathrm{Pb}}$ is defined as the ratio of differential cross-sections

$$R_{p\mathrm{Pb}}(p_{\mathrm{T}}, y^*) \equiv \frac{1}{A} \frac{\mathrm{d}^2\sigma_{p\mathrm{Pb}}(p_{\mathrm{T}}, y^*)/(\mathrm{d}p_{\mathrm{T}}\mathrm{d}y^*)}{\mathrm{d}^2\sigma_{pp}(p_{\mathrm{T}}, y^*)/(\mathrm{d}p_{\mathrm{T}}\mathrm{d}y^*)}, \tag{2}$$

where $A = 208$ is the lead nucleus mass number and σ_{pp} is the prompt $D^+_{(s)}$ meson cross-section in pp collisions at $\sqrt{s} = 8.16\,\mathrm{TeV}$. The latter are obtained by an interpolation between LHCb measurements at $\sqrt{s} = 5.02\,\mathrm{TeV}$ and $\sqrt{s} = 13\,\mathrm{TeV}$ [47, 48]. The interpolation is performed within the common kinematic range $1 < p_\mathrm{T} < 10\,\mathrm{GeV}/c$ and $2.0 < y < 4.5$, using a power-law function. The difference obtained when using a linear function is assigned as a systematic uncertainty.

The nuclear modification factors for $D^+_{(s)}$ mesons as a function of p_T are displayed in Fig. 1, where the results are integrated over the rapidity range $2.0 < y^* < 4.0$ for the forward rapidity region and $-4.5 < y^* < -2.5$ for the backward region. A significant suppression of $D^+_{(s)}$ production in $p\mathrm{Pb}$ collisions, with respect to those in pp collisions scaled by the lead mass number, is observed at forward rapidity. Figures showing $R_{p\mathrm{Pb}}$ in different y^* intervals of width $\Delta y^* = 0.5$, as well as the numerical values, are given in the Supplemental Material [41].

The $R_{p\mathrm{Pb}}$ results are compared with nPDF theoretical calculations. These calculations use the HELAC-Onia approach [49, 50], which is based on a data-driven modeling of the scattering at partonic level folded with free proton PDFs [51]. They are first tuned by fitting the cross-sections measured in pp collisions at the LHC. Then, the modified PDFs of nucleons in the Pb nucleus are introduced to calculate the cross-sections in $p\mathrm{Pb}$ collisions and to estimate the effect of nPDFs. Reweighted EPPS16 [52] or nCTEQ15 [53] nPDF sets, which incorporate LHC heavy-flavor data [54–57] in a Bayesian-reweighting analysis [58], are used in these calculations. This procedure leads to considerably reduced uncertainties with respect to calculations using the default nPDFs. The theoretical uncertainties shown in Fig. 1 are dominated by the nPDF parameterisations and correspond to a 68% confidence interval. At forward rapidity, the calculations are in satisfactory agreement with data. At backward rapidity, the data are lower than the calculations, indicating a weaker antishadowing effect or possible final-state effects that depend weakly on charm hadronization.

The nuclear modification factors in the forward rapidity region (small momentum fraction x) are also compared with two calculations based on the CGC effective field theory, CGC1 [59, 60] and CGC2 [61]. The most significant theoretical uncertainty in CGC2 is the initial saturation scale of the target nucleus. The CGC1 predictions have much smaller uncertainties than the CGC2 predictions, as they include only variations of the charm quark mass and of the factorisation scale, which largely cancel out in the $R_{p\mathrm{Pb}}$ ratio. The CGC1 calculations are consistent with the upper bound of the CGC2 predictions and slightly overshoot the data. The CGC2 predictions show a stronger suppression than HELAC-Onia, especially for $p_\mathrm{T} < 3\,\mathrm{GeV}/c$.

The forward-backward cross-section ratio R_{FB} is defined as

$$R_{\mathrm{FB}}(p_\mathrm{T}, |y^*|) = \frac{\mathrm{d}^2\sigma_{p\mathrm{Pb}}(p_\mathrm{T}, +|y^*|)/(\mathrm{d}p_\mathrm{T}\mathrm{d}y^*)}{\mathrm{d}^2\sigma_{\mathrm{Pb}p}(p_\mathrm{T}, -|y^*|)/(\mathrm{d}p_\mathrm{T}\mathrm{d}y^*)} \,, \tag{3}$$

and calculated in the common $|y^*|$ interval of the forward-backward acceptances, namely $2.5 < |y^*| < 4$. The measurements of R_{FB} are shown as a function of p_T and $|y^*|$ in Fig. 2, along with the nPDF calculations [52, 53]. Good agreement with nPDF calculations is found at low p_T, however, the data show a clear rising trend with increasing p_T, reaching unity at the highest p_T values. This is in contrast to the nPDF calculations, which predict $R_{\mathrm{FB}} \sim 0.7$ almost independently of p_T. This discrepancy originates from the observed suppression of high-p_T $D^+_{(s)}$ mesons at backward rapidity.
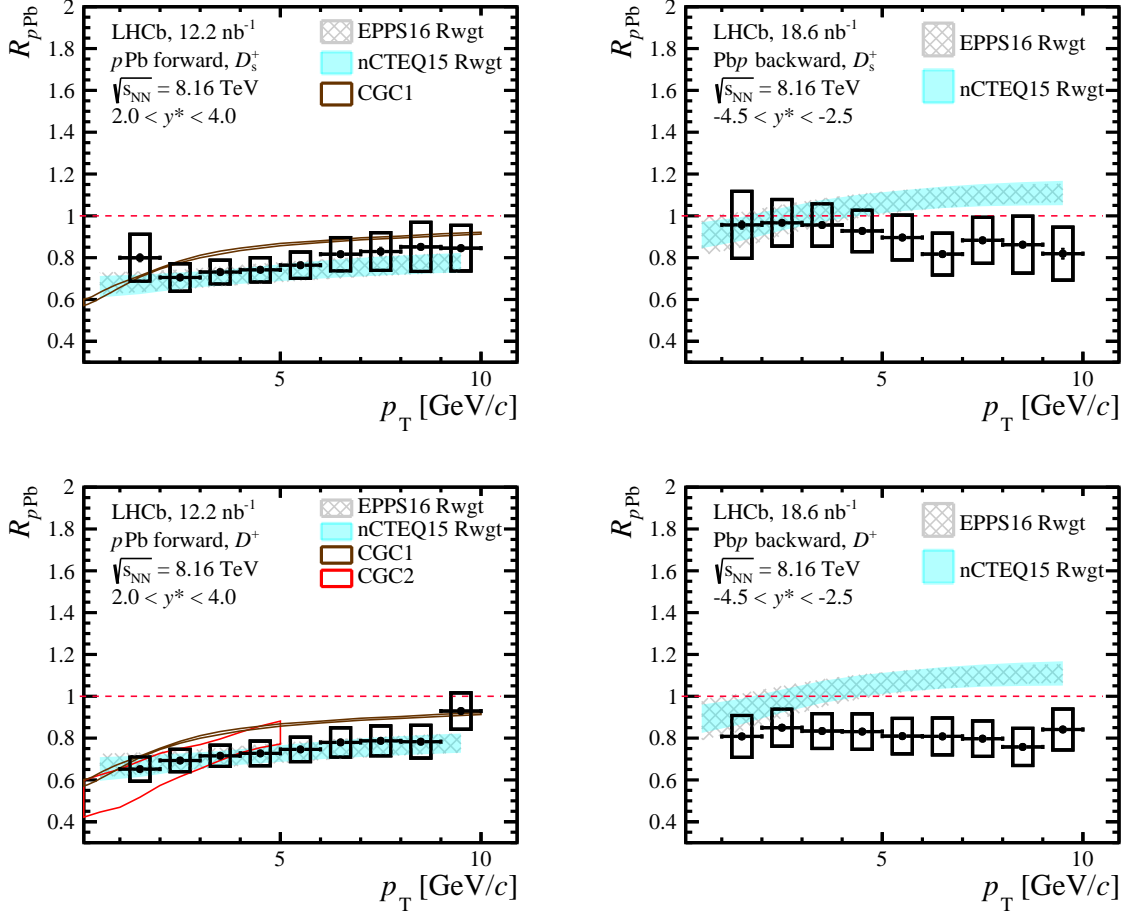
Figure 1: Nuclear modification factor $R_{p\mathrm{Pb}}$ as a function of p_T for prompt (upper) D_s^+ and (lower) D^+ mesons. Forward rapidity results are shown on the left and backward rapidity on the right. The vertical error bars show the statistical uncertainties and the boxes show the systematic uncertainties. The theoretical calculations are also shown [52, 53, 59–61].

The cross-section ratio $\sigma_{D_s^+}/\sigma_{D^+}$, which is written as

$$\frac{\sigma_{D_s^+}}{\sigma_{D^+}} = \frac{N_{D_s^+}}{N_{D^+}} \times \frac{\mathcal{B}_{D^+}}{\mathcal{B}_{D_s^+}} \times \frac{\epsilon_{D^+}^{\mathrm{acc}}}{\epsilon_{D_s^+}^{\mathrm{acc}}} \times \frac{\epsilon_{D^+}^{\mathrm{trig}}}{\epsilon_{D_s^+}^{\mathrm{trig}}} \times \frac{\epsilon_{D^+}^{\mathrm{PID}}}{\epsilon_{D_s^+}^{\mathrm{PID}}} \times \frac{\epsilon_{D^+}^{\mathrm{rec\&sel}}}{\epsilon_{D_s^+}^{\mathrm{rec\&sel}}}, \qquad (4)$$

is more precisely measured thanks to a cancellation of systematic uncertainties. The dependence of $\sigma_{D_s^+}/\sigma_{D^+}$ versus the primary charged particle multiplicity is measured in the $D_{(s)}^+$ kinematic intervals $2 < p_\mathrm{T} < 12\,\mathrm{GeV}/c$ and $1.8 < y^* < 3.3$ $(-4.3 < y^* < -2.8)$ for forward (backward) rapidity. The primary charged particle multiplicity, denoted as N_{ch}, represents the number of charged particles originating from the collisions, including decay products. In this Letter, it is estimated within the forward-pseudorapidity region $(2 < \eta < 4.8)$ by measuring the number of tracks used to reconstruct the primary vertex, denoted as $N_{\mathrm{Tracks}}^{\mathrm{PV}}$. The correlation between the measured $N_{\mathrm{Tracks}}^{\mathrm{PV}}$ and N_{ch} is obtained from simulation.

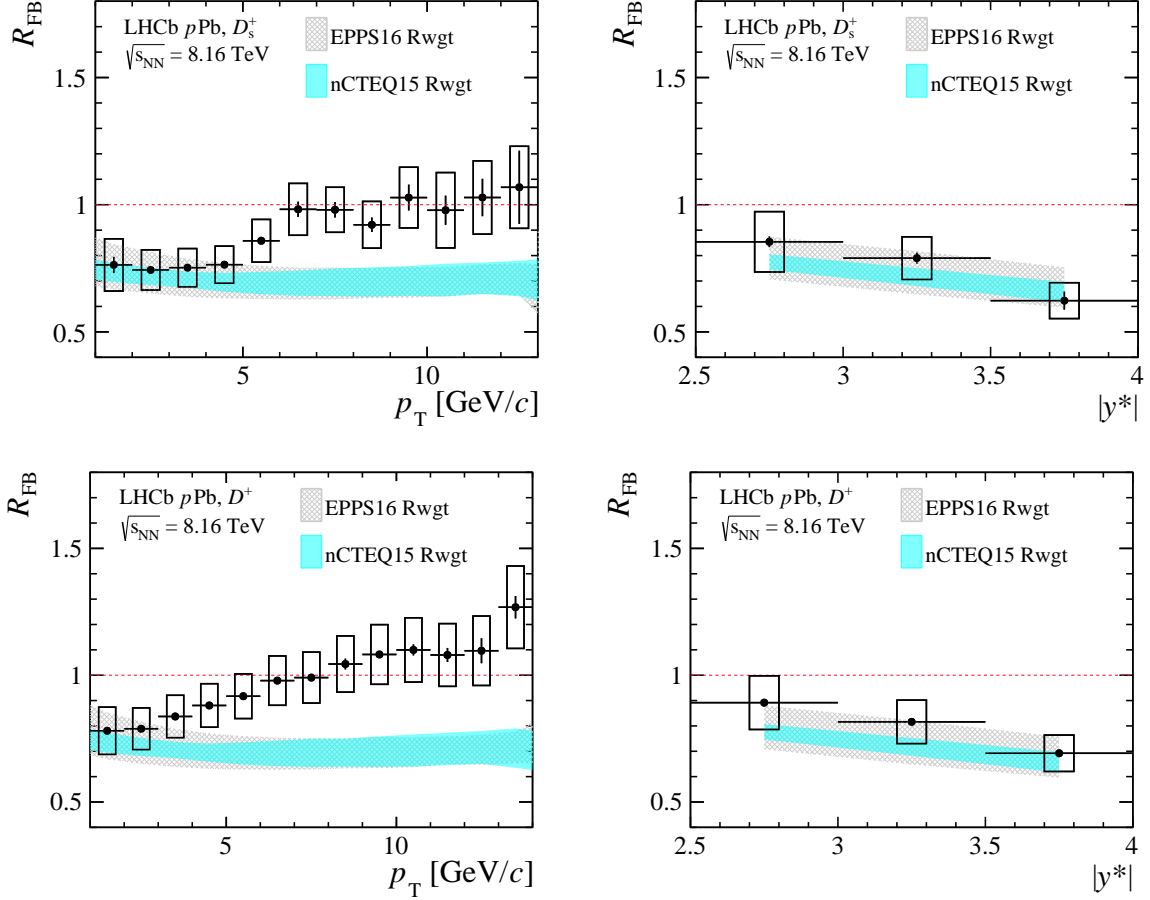Figure 3 shows the dependence of $\sigma_{D_s^+}/\sigma_{D^+}$ on primary charged particle multiplicity

Figure 2: Forward-backward cross-section ratio R_{FB} for prompt (upper) D_s^+ and (lower) D^+ mesons as a function of (left) p_{T} and (right) y^*. The vertical error bars show the statistical uncertainties and the boxes show the systematic uncertainties. The coloured bands represent the theoretical calculations, incorporating nPDFs EPPS16 (gray) [52] and nCTEQ15 (cyan) [53].

in four different p_{T} intervals (integrated over rapidity). Plots of $\sigma_{D_s^+}/\sigma_{D^+}$ in different y^* intervals and the derived numerical values are given in the Supplemental Material [41]. These measurements show that the $\sigma_{D_s^+}/\sigma_{D^+}$ ratio increases significantly as a function of the primary charged particle multiplicity, especially in the low-p_{T} and backward rapidity regions. They deviate from a flat distribution, expected if only the fragmentation mechanism is considered, by 6.1 ($2 < p_{\mathrm{T}} < 4\,\mathrm{GeV}/c$), 6.8 ($4 < p_{\mathrm{T}} < 6\,\mathrm{GeV}/c$), 2.7 ($6 < p_{\mathrm{T}} < 8\,\mathrm{GeV}/c$) and 3.2 ($8 < p_{\mathrm{T}} < 12\,\mathrm{GeV}/c$) standard deviations in the forward rapidity region, and by 7.9 ($2 < p_{\mathrm{T}} < 4\,\mathrm{GeV}/c$), 10.5 ($4 < p_{\mathrm{T}} < 6\,\mathrm{GeV}/c$), 4.4 ($6 < p_{\mathrm{T}} < 8\,\mathrm{GeV}/c$) and 1.1 ($8 < p_{\mathrm{T}} < 12\,\mathrm{GeV}/c$) standard deviations at backward rapidity. As a comparison, the measured $\sigma_{D_s^+}/\sigma_{D^+}$ ratios in e^+e^- [62], pp [10,63], pPb [64] and PbPb [65] collisions are also shown in the Fig. 3. There are significant differences in the $\sigma_{D_s^+}/\sigma_{D^+}$ ratios between pp and PbPb collisions. The LHCb measurements reveal a trend where the ratio tends to resemble that of pp collisions in low-multiplicity pPb collisions, while it converges towards the behavior observed in PbPb collisions in high-multiplicity pPb collisions. In pPb collisions, the LHCb data are compatible with the ratio measured by ALICE within uncertainties. The $\sigma_{D_s^+}/\sigma_{D^+}$ pattern is similar in both the forward
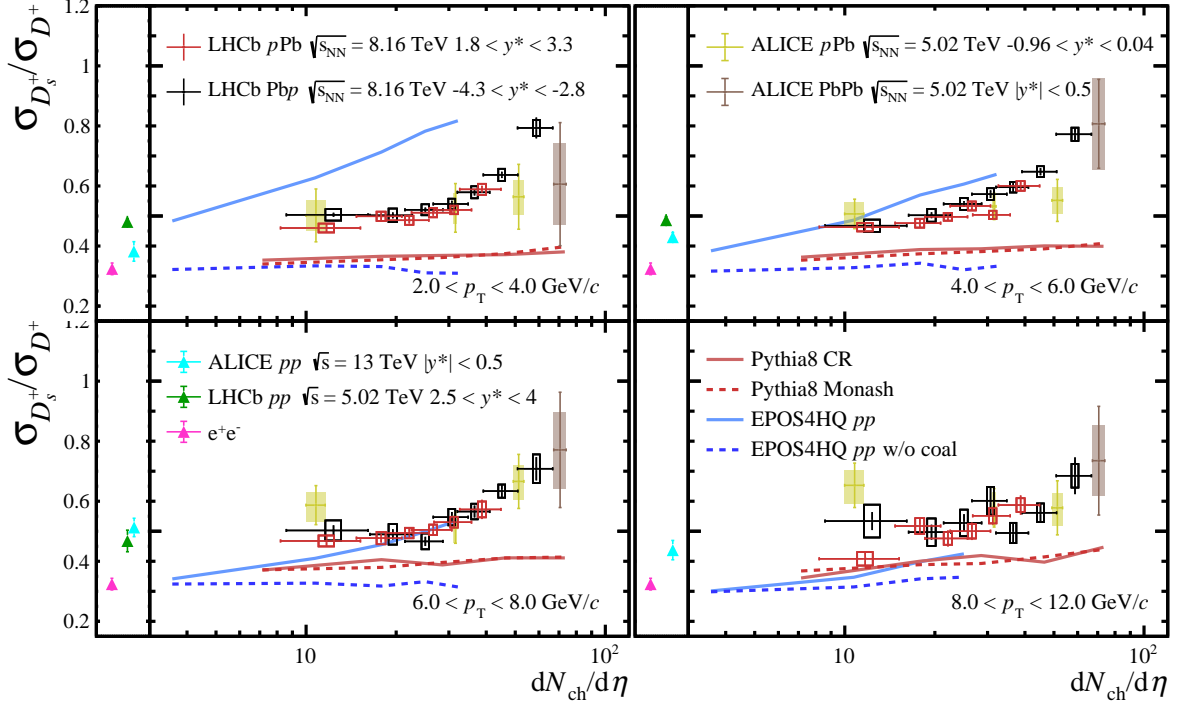
Figure 3: Cross-section ratio $\sigma_{D_s^+}/\sigma_{D^+}$ versus the primary charged particles per unit of pseudorapidity in e^+e^- [62], pp [10,63], pPb [64], PbPb [65] collisions in different $D_{(s)}^+$ p_T ranges. The vertical error bars show the statistical uncertainties and the boxes show the systematic uncertainties. The colored bands contain both statistical and systematic uncertainties. The calculations from Pythia 8 [66,67], EPOS4HQ [68,69] and EPOS4HQ without coalescence mechanism are also shown. These calculations are applicable to pp collisions at $\sqrt{s} = 8.16\,\mathrm{TeV}$ within the rapidity range of $1.8 < y^* < 3.3$.

and backward rapidity regions. This suggests that the $\sigma_{D_s^+}/\sigma_{D^+}$ ratio is independent of rapidity, and the mechanism contributing to this ratio increase is strongly correlated with the charged particle density. Additionally, theoretical calculations are compared using PYTHIA 8 with Monash [66] and CR [67] tunes, along with EPOS4HQ [68,69]. EPOS4HQ extends the EPOS4 framework to include heavy quarks and incorporates a coalescence mechanism in hadronization. These calculations are applicable to pp collisions. Theoretical calculations from Pythia 8 underestimate experimental measurements and and do not fully capture the trends dependent on multiplicity. While EPOS4HQ also exhibits some discrepancies with experimental data, it can depict the multiplicity-dependent trends across all p_T intervals by introducing a coalescence mechanism.

In summary, the prompt $D_{(s)}^+$ production cross-sections are measured by the LHCb experiment in pPb collisions at $\sqrt{s_{NN}} = 8.16\,\mathrm{TeV}$, both in the forward and backward rapidity regions. The nuclear modification factors are measured and found to be consistent with the previous results with D^0 mesons [7]. The results show a strong suppression of the $D_{(s)}^+$ cross-sections at forward rapidity, consistent with the nPDF and CGC effective theory calculations. At backward rapidity, the $R_{p\mathrm{Pb}}$ values of $D_{(s)}^+$ mesons are lower than nPDF calculations at high p_T, indicating a weaker antishadowing effect than predicted by the models or additional hadronization-independent final-state effects. Moreover, the

forward-backward cross-section ratio also shows a deviation from the nPDF calculations at high p_{T}. Combined with the nuclear modification factors, this deviation may arise from the observed suppression of high-p_{T} $D^+_{(s)}$ mesons at backward rapidity. The production of D^+_s mesons is significantly enhanced relative to D^+ mesons in high particle multiplicity proton-lead collision events, in particular for low p_{T} and backward rapidity. This is the first observation of strangeness enhancement in charm quark hadronization in high-multiplicity small collision systems. The multiplicity-dependent trend is well understood within EPOS4HQ.

Acknowledgements

Supplemental material

The multiplicity variable used in this paper is the number of tracks used to reconstruct the primary vertex (PV), $N_{\text{Tracks}}^{\text{PV}}$. The $N_{\text{Tracks}}^{\text{PV}}$ distribution is affected by the position of the primary vertex along the beam axis. This is due to the asymmetry of the pPb collisions and the pseudorapidity coverage limitations of vertex locator (VELO). To address this effect, a selection is made on the position of the primary vertex along the beam axis to ensure the stable distribution of $N_{\text{Tracks}}^{\text{PV}}$ within this range. The $N_{\text{Tracks}}^{\text{PV}}$ distributions for three categories of events, namely minimum-bias events, D_s^+ signal events, and D^+ signal events, with the additional requirement of one reconstructed primary vertex for each category, are shown in Fig. 4. The multiplicity distributions for D_s^+ and D^+ signal events are extracted from data; background is removed using the *sPlot* method [36].

The $\sigma_{D_s^+}/\sigma_{D^+}$ ratios are extracted in different multiplicity classes defined as 10-60, 60-80, 80-100, 100-120, 120-140, 140-200 (10-60, 60-80, 80-100, 100-120, 120-140, 140-180, 180-250) $N_{\text{Tracks}}^{\text{PV}}$ for forward (backward) rapidity region. The normalised multiplicity is defined as $N_{\text{Tracks}}^{\text{PV}}/\langle N_{\text{Tracks}}^{\text{PV}}\rangle_{\text{MB}}$, where $\langle N_{\text{Tracks}}^{\text{PV}}\rangle_{\text{MB}}$ is the average multiplicity for MB events in the corresponding beam configuration. For the forward (backward) rapidity sample $\langle N_{\text{Tracks}}^{\text{PV}}\rangle_{\text{MB}} = 60.3\ (69.0)$ with negligible uncertainty. The primary charged particles per unity of pseudorapidity is defined as $\mathrm{d}N_{\text{ch}}/\mathrm{d}\eta$, where η range from 2 to 4.8. The primary charged particle multiplicity, denoted as N_{ch}, represents the number of charged particles originating from the collisions, including decay products. It is estimated within the forward-pseudorapidity region ($2 < \eta < 4.8$) by measuring $N_{\text{Tracks}}^{\text{PV}}$. In the forward (backward) rapidity region, the means and standard deviations of N_{ch} in different $N_{\text{Tracks}}^{\text{PV}}$ intervals are denoted as 32.8 ± 9.8, 49.9 ± 8.6, 61.9 ± 10.0, 74.5 ± 11.4, 87.5 ± 12.5, 108.4 ± 17.0 (34.6 ± 10.5, 54.6 ± 8.8, 70.1 ± 10.2, 86.0 ± 11.5, 102.3 ± 12.7, 126.2 ± 16.7, 164.7 ± 22.1).
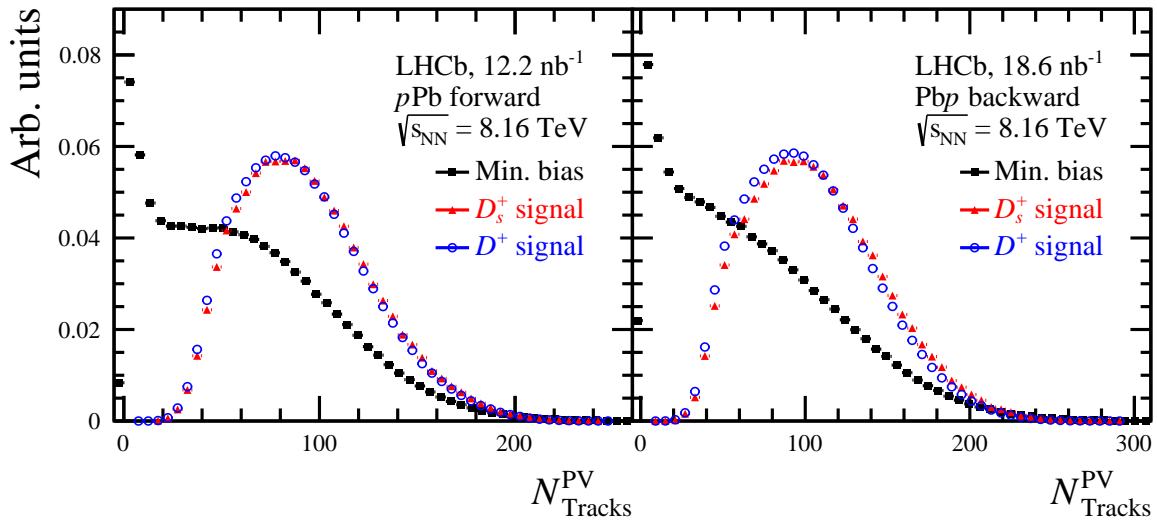

Figure 4: Distribution of the number of charged tracks used to reconstruct the PV for $D_{(s)}^+$ signal and minimum-bias events in (left) forward and (right) backward configurations, each with only one primary vertex. The vertical scale is arbitrary.

The results of the fits to the invariant-mass and $\log_{10}(\chi_{\text{IP}}^2)$ distributions in the forward

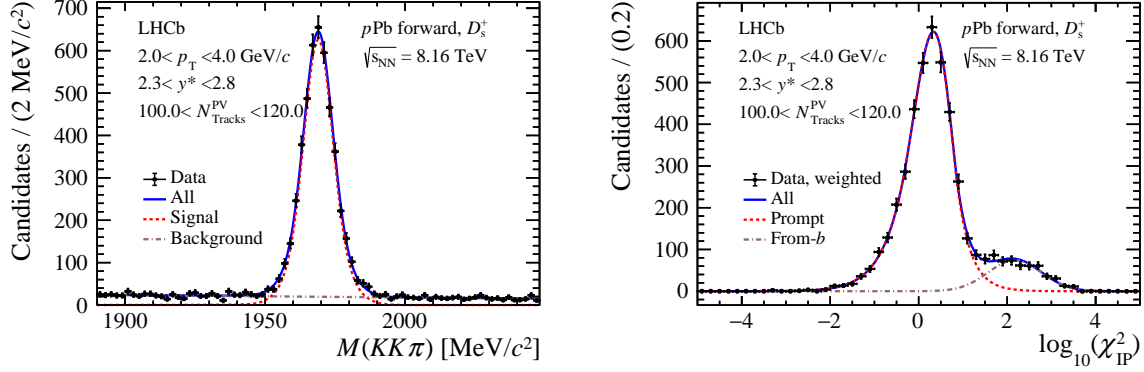and backward rapidity intervals are shown in Fig. 5–8.

Figure 5: Distributions of (left) $M(KK\pi)$ and (right) $\log_{10}(\chi^2_{\mathrm{IP}})$ for inclusive D_s^+ mesons in the forward data sample in the interval of $2.0 < p_{\mathrm{T}} < 4.0\,\mathrm{GeV}/c$, $2.3 < y^* < 2.8$ and $100 < N_{\mathrm{Tracks}}^{\mathrm{PV}} < 120$. The fit results are overlaid. For the $\log_{10}(\chi^2_{\mathrm{IP}})$ fit, the data are weighted using the *sPlot* method to subtract the background component.
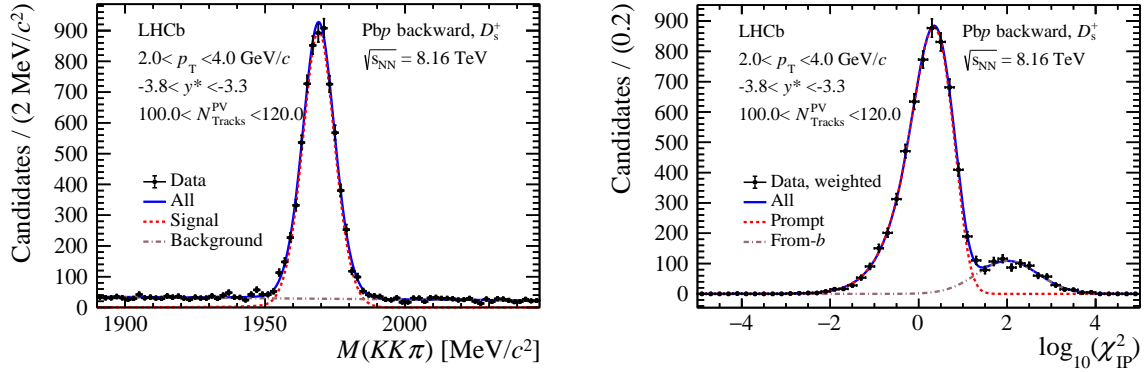

Figure 6: Distributions of (left) $M(KK\pi)$ and (right) $\log_{10}(\chi^2_{\mathrm{IP}})$ for inclusive D_s^+ mesons in the backward data sample in the interval of $2.0 < p_{\mathrm{T}} < 4.0\,\mathrm{GeV}/c$, $-3.8 < y^* < -3.3$ and $100 < N_{\mathrm{Tracks}}^{\mathrm{PV}} < 120$. The fit results are overlaid. For the $\log_{10}(\chi^2_{\mathrm{IP}})$ fit, the data are weighted using the *sPlot* method to subtract the background component.

The differential cross-section for prompt D_s^+ and D^+ mesons in both forward and backward rapidities are shown in Fig. 9–12. The corresponding numerical values are listed in Tables 2–7.

The nuclear modification factor $R_{p\mathrm{Pb}}$ for prompt D_s^+ and D^+ mesons in both forward and backward rapidities are shown in Fig. 13–15. The corresponding numerical values are listed in Tables 8–13.

The numerical values for the forward and backward production ratio R_{FB} of prompt D_s^+ and D^+ mesons are given in Tables 14 and 15.

The production cross-section ratio of D_s^+ over D^+ mesons $\sigma_{D_s^+}/\sigma_{D^+}$ in both forward and backward rapidities are shown in Fig. 16–18. The corresponding numerical values are listed in Tables 16 and 17.
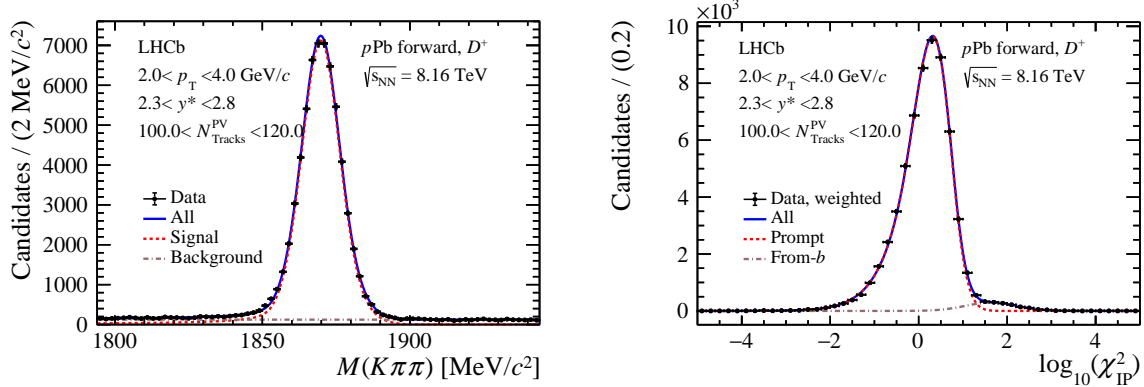
Figure 7: Distributions of (left) $M(K\pi\pi)$ and (right) $\log_{10}(\chi^2_{\mathrm{IP}})$ for inclusive D^+ mesons in the forward data sample in the interval of $2.0 < p_{\mathrm{T}} < 4.0\,\mathrm{GeV}/c$, $2.3 < y^* < 2.8$ and $100 < N^{\mathrm{PV}}_{\mathrm{Tracks}} < 120$. The fit results are overlaid. For the $\log_{10}(\chi^2_{\mathrm{IP}})$ fit, the data are weighted using the *sPlot* method to subtract the background component.

Figure 8: Distributions of (left) $M(K\pi\pi)$ and (right) $\log_{10}(\chi^2_{\mathrm{IP}})$ for inclusive D^+ mesons in the backward data sample in the interval of $2.0 < p_{\mathrm{T}} < 4.0\,\mathrm{GeV}/c$, $-3.8 < y^* < -3.3$ and $100 < N^{\mathrm{PV}}_{\mathrm{Tracks}} < 120$. The fit results are overlaid. For the $\log_{10}(\chi^2_{\mathrm{IP}})$ fit, the data are weighted using the *sPlot* method to subtract the background component.
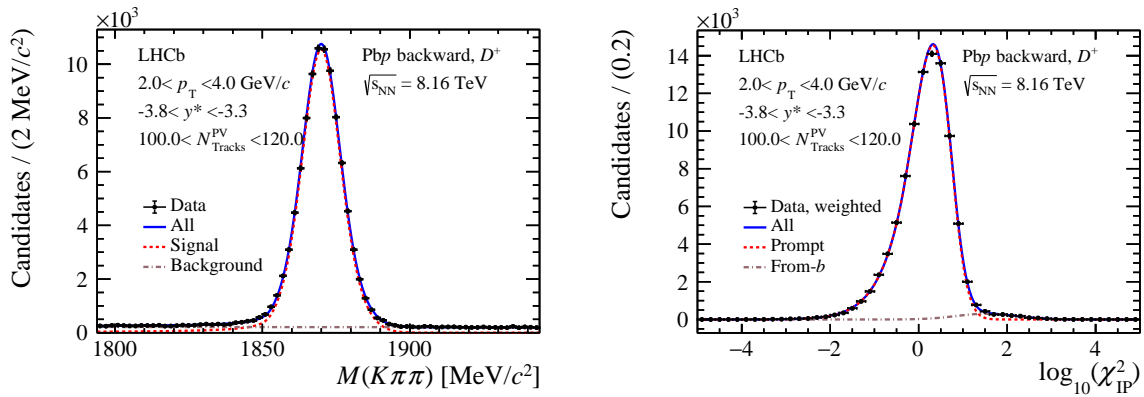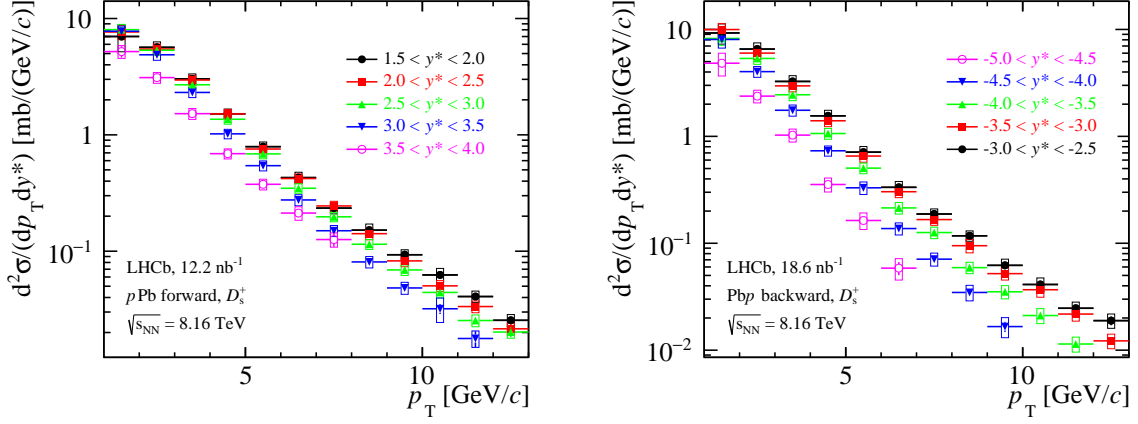
11

Figure 9: Double-differential cross-section of prompt D_s^+ production in pPb collisions at (left) forward and (right) backward rapidities. The vertical error bars show the statistical uncertainties and the boxes show the systematic uncertainties.

Figure 10: Double-differential cross-section of prompt D^+ production in pPb collisions at (left) forward and (right) backward rapidities. The vertical error bars show the statistical uncertainties and the boxes show the systematic uncertainties.
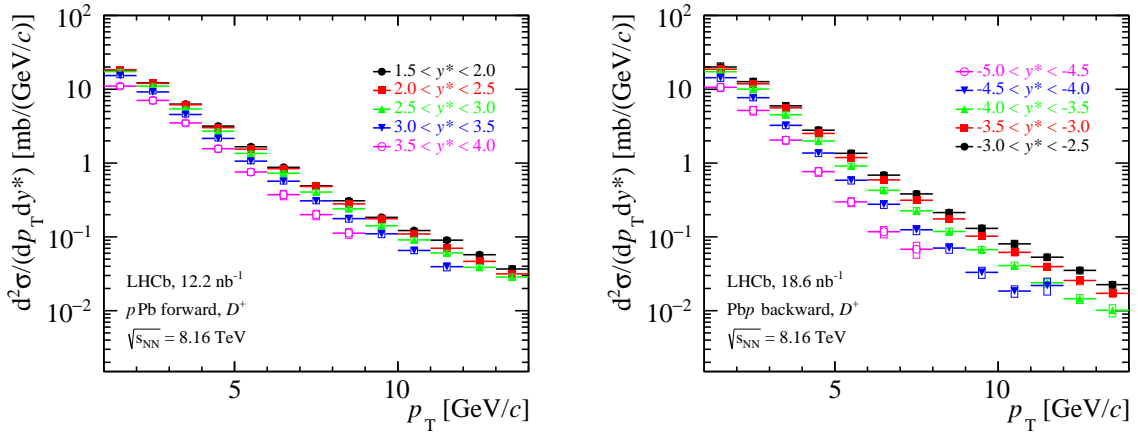
Figure 11: Differential cross-section of prompt D_s^+ production in pPb collisions as a function of (left) p_{T} and (right) y^*. The vertical error bars show the statistical uncertainties and the boxes show the systematic uncertainties.

Figure 12: Differential cross-section of prompt D^+ production in pPb collisions as a function of (left) p_{T} and (right) y^*. The vertical error bars show the statistical uncertainties and the boxes show the systematic uncertainties.

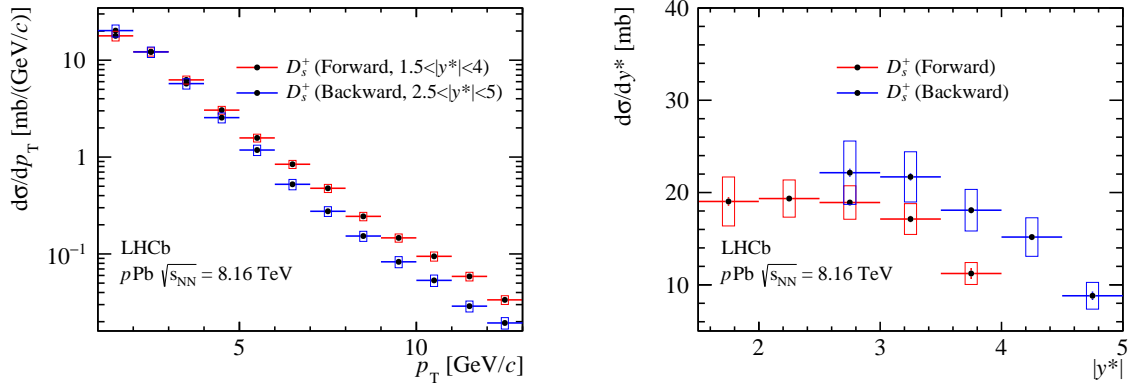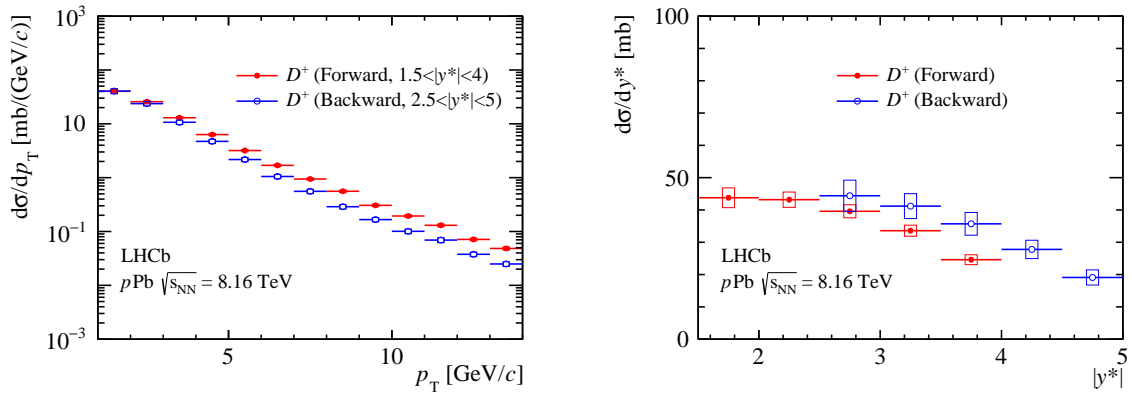Table 2: Double-differential cross-section for prompt D_s^+ production as a function of p_T and y^* in pPb collisions at forward and backward rapidities. The first uncertainty is statistical, the second the component of the systematic uncertainty that is uncorrelated between bins and the third the correlated systematic component.

p_T [GeV/c]\y^*	$d^2\sigma/(dp_Tdy^*)$ [mb/(GeV/c)] (Forward)				
	[1.5, 2]	[2, 2.5]	[2.5, 3]	[3, 3.5]	[3.5, 4]
[1, 2]	7.006 ± 0.422 ± 1.613 ± 0.861	7.658 ± 0.220 ± 0.745 ± 0.775	8.021 ± 0.270 ± 0.441 ± 0.763	7.770 ± 0.334 ± 0.389 ± 0.733	5.197 ± 0.583 ± 0.378 ± 0.536
[2, 3]	5.653 ± 0.156 ± 0.157 ± 0.625	5.464 ± 0.049 ± 0.244 ± 0.520	5.337 ± 0.048 ± 0.187 ± 0.485	4.877 ± 0.073 ± 0.212 ± 0.456	3.105 ± 0.093 ± 0.149 ± 0.296
[3, 4]	3.027 ± 0.120 ± 0.051 ± 0.310	2.961 ± 0.042 ± 0.094 ± 0.273	2.694 ± 0.026 ± 0.034 ± 0.245	2.314 ± 0.032 ± 0.064 ± 0.215	1.521 ± 0.055 ± 0.074 ± 0.146
[4, 5]	1.518 ± 0.029 ± 0.026 ± 0.147	1.514 ± 0.020 ± 0.020 ± 0.137	1.362 ± 0.015 ± 0.030 ± 0.123	1.020 ± 0.024 ± 0.013 ± 0.095	0.689 ± 0.028 ± 0.017 ± 0.066
[5, 6]	0.792 ± 0.022 ± 0.017 ± 0.075	0.755 ± 0.014 ± 0.012 ± 0.068	0.686 ± 0.010 ± 0.014 ± 0.062	0.543 ± 0.011 ± 0.016 ± 0.051	0.376 ± 0.016 ± 0.014 ± 0.037
[6, 7]	0.429 ± 0.012 ± 0.026 ± 0.041	0.421 ± 0.005 ± 0.011 ± 0.038	0.347 ± 0.006 ± 0.008 ± 0.031	0.276 ± 0.011 ± 0.015 ± 0.026	0.213 ± 0.016 ± 0.018 ± 0.022
[7, 8]	0.235 ± 0.008 ± 0.012 ± 0.022	0.245 ± 0.005 ± 0.007 ± 0.022	0.197 ± 0.005 ± 0.004 ± 0.018	0.150 ± 0.007 ± 0.008 ± 0.014	0.126 ± 0.017 ± 0.011 ± 0.014
[8, 9]	0.152 ± 0.011 ± 0.013 ± 0.014	0.141 ± 0.004 ± 0.010 ± 0.013	0.115 ± 0.003 ± 0.004 ± 0.010	0.081 ± 0.004 ± 0.004 ± 0.008	–
[9, 10]	0.093 ± 0.008 ± 0.004 ± 0.009	0.083 ± 0.002 ± 0.005 ± 0.008	0.069 ± 0.002 ± 0.003 ± 0.006	0.048 ± 0.003 ± 0.003 ± 0.005	–
[10, 11]	0.063 ± 0.003 ± 0.006 ± 0.006	0.050 ± 0.002 ± 0.003 ± 0.005	0.044 ± 0.002 ± 0.002 ± 0.004	0.032 ± 0.003 ± 0.007 ± 0.003	–
[11, 12]	0.041 ± 0.002 ± 0.002 ± 0.004	0.033 ± 0.001 ± 0.002 ± 0.003	0.025 ± 0.001 ± 0.002 ± 0.002	0.018 ± 0.003 ± 0.002 ± 0.002	–
[12, 13]	0.025 ± 0.001 ± 0.002 ± 0.002	0.022 ± 0.002 ± 0.002 ± 0.002	0.020 ± 0.002 ± 0.001 ± 0.002	–	–

p_T [GeV/c]\y^*	$d^2\sigma/(dp_Tdy^*)$ [mb/(GeV/c)] (Backward)				
	[−3, −2.5]	[−3.5, −3]	[−4, −3.5]	[−4.5, −4]	[−5, −4.5]
[1, 2]	9.278 ± 0.410 ± 1.364 ± 1.446	9.981 ± 0.361 ± 0.477 ± 1.269	8.240 ± 0.334 ± 0.392 ± 1.070	8.061 ± 0.321 ± 0.699 ± 1.180	4.832 ± 0.441 ± 1.035 ± 0.526
[2, 3]	6.553 ± 0.128 ± 0.205 ± 0.913	6.009 ± 0.135 ± 0.244 ± 0.726	5.355 ± 0.054 ± 0.125 ± 0.626	4.031 ± 0.065 ± 0.137 ± 0.446	2.379 ± 0.120 ± 0.136 ± 0.293
[3, 4]	3.264 ± 0.032 ± 0.101 ± 0.420	2.965 ± 0.071 ± 0.047 ± 0.356	2.449 ± 0.043 ± 0.043 ± 0.289	1.754 ± 0.024 ± 0.052 ± 0.203	1.027 ± 0.039 ± 0.067 ± 0.125
[4, 5]	1.556 ± 0.037 ± 0.034 ± 0.194	1.399 ± 0.015 ± 0.026 ± 0.165	1.063 ± 0.022 ± 0.022 ± 0.122	0.733 ± 0.009 ± 0.021 ± 0.077	0.355 ± 0.016 ± 0.027 ± 0.046
[5, 6]	0.712 ± 0.021 ± 0.022 ± 0.089	0.654 ± 0.008 ± 0.020 ± 0.079	0.504 ± 0.007 ± 0.011 ± 0.056	0.330 ± 0.010 ± 0.018 ± 0.041	0.163 ± 0.011 ± 0.017 ± 0.023
[6, 7]	0.334 ± 0.014 ± 0.018 ± 0.041	0.304 ± 0.004 ± 0.008 ± 0.036	0.214 ± 0.005 ± 0.007 ± 0.026	0.137 ± 0.004 ± 0.007 ± 0.016	0.059 ± 0.008 ± 0.011 ± 0.008
[7, 8]	0.188 ± 0.005 ± 0.006 ± 0.021	0.167 ± 0.004 ± 0.006 ± 0.019	0.126 ± 0.003 ± 0.005 ± 0.015	0.071 ± 0.003 ± 0.004 ± 0.009	–
[8, 9]	0.117 ± 0.004 ± 0.005 ± 0.012	0.095 ± 0.002 ± 0.005 ± 0.013	0.059 ± 0.005 ± 0.003 ± 0.007	0.035 ± 0.002 ± 0.004 ± 0.005	–
[9, 10]	0.062 ± 0.003 ± 0.003 ± 0.008	0.052 ± 0.002 ± 0.003 ± 0.006	0.035 ± 0.001 ± 0.002 ± 0.004	0.017 ± 0.002 ± 0.003 ± 0.002	–
[10, 11]	0.041 ± 0.002 ± 0.003 ± 0.005	0.037 ± 0.001 ± 0.003 ± 0.004	0.021 ± 0.001 ± 0.002 ± 0.003	0.008 ± 0.002 ± 0.002 ± 0.001	–
[11, 12]	0.025 ± 0.001 ± 0.002 ± 0.003	0.022 ± 0.001 ± 0.002 ± 0.003	0.011 ± 0.001 ± 0.001 ± 0.001	–	–
[12, 13]	0.019 ± 0.002 ± 0.002 ± 0.002	0.012 ± 0.001 ± 0.001 ± 0.002	0.008 ± 0.001 ± 0.001 ± 0.001	–	–

Table 3: Double-differential cross-section for prompt D^+ production as a function of p_T and y^* in pPb collisions at forward and backward rapidities. The first uncertainty is statistical, the second the component of the systematic uncertainty that is uncorrelated between bins and the third the correlated systematic component.

$d^2\sigma/(dp_T dy^*)$ [mb/(GeV/c)] (Forward)

p_T[GeV/c]\y^*	[1.5, 2]	[2, 2.5]	[2.5, 3]	[3, 3.5]	[3.5, 4]
[1, 2]	18.276 ± 0.305 ± 0.884 ± 1.481	18.390 ± 0.095 ± 0.563 ± 1.209	17.369 ± 0.020 ± 0.607 ± 1.013	15.329 ± 0.080 ± 0.439 ± 0.885	11.032 ± 0.108 ± 0.632 ± 0.631
[2, 3]	12.215 ± 0.059 ± 0.364 ± 0.886	12.020 ± 0.024 ± 0.352 ± 0.701	11.018 ± 0.083 ± 0.372 ± 0.597	9.205 ± 0.026 ± 0.260 ± 0.506	7.066 ± 0.035 ± 0.608 ± 0.400
[3, 4]	6.286 ± 0.025 ± 0.171 ± 0.414	6.172 ± 0.014 ± 0.174 ± 0.343	5.410 ± 0.010 ± 0.141 ± 0.290	4.552 ± 0.010 ± 0.231 ± 0.249	3.498 ± 0.020 ± 0.245 ± 0.198
[4, 5]	3.168 ± 0.014 ± 0.086 ± 0.192	3.020 ± 0.005 ± 0.154 ± 0.161	2.708 ± 0.009 ± 0.103 ± 0.145	2.160 ± 0.008 ± 0.117 ± 0.118	1.566 ± 0.014 ± 0.133 ± 0.092
[5, 6]	1.664 ± 0.008 ± 0.047 ± 0.097	1.543 ± 0.005 ± 0.046 ± 0.082	1.350 ± 0.005 ± 0.062 ± 0.072	1.062 ± 0.005 ± 0.062 ± 0.059	0.757 ± 0.009 ± 0.065 ± 0.046
[6, 7]	0.876 ± 0.018 ± 0.024 ± 0.050	0.840 ± 0.004 ± 0.041 ± 0.045	0.730 ± 0.004 ± 0.031 ± 0.039	0.568 ± 0.004 ± 0.037 ± 0.032	0.373 ± 0.015 ± 0.049 ± 0.024
[7, 8]	0.491 ± 0.005 ± 0.014 ± 0.028	0.482 ± 0.003 ± 0.017 ± 0.026	0.405 ± 0.002 ± 0.019 ± 0.022	0.308 ± 0.003 ± 0.021 ± 0.018	0.200 ± 0.008 ± 0.026 ± 0.014
[8, 9]	0.308 ± 0.000 ± 0.013 ± 0.018	0.280 ± 0.002 ± 0.009 ± 0.015	0.240 ± 0.002 ± 0.011 ± 0.013	0.177 ± 0.003 ± 0.015 ± 0.011	0.112 ± 0.010 ± 0.014 ± 0.009
[9, 10]	0.184 ± 0.000 ± 0.007 ± 0.011	0.176 ± 0.001 ± 0.007 ± 0.010	0.141 ± 0.002 ± 0.007 ± 0.008	0.110 ± 0.002 ± 0.010 ± 0.007	—
[10, 11]	0.122 ± 0.002 ± 0.004 ± 0.007	0.110 ± 0.002 ± 0.004 ± 0.006	0.091 ± 0.001 ± 0.005 ± 0.005	0.066 ± 0.002 ± 0.005 ± 0.004	—
[11, 12]	0.090 ± 0.001 ± 0.004 ± 0.005	0.070 ± 0.001 ± 0.004 ± 0.004	0.061 ± 0.001 ± 0.004 ± 0.004	0.039 ± 0.002 ± 0.004 ± 0.003	—
[12, 13]	0.057 ± 0.001 ± 0.003 ± 0.003	0.047 ± 0.001 ± 0.002 ± 0.003	0.039 ± 0.001 ± 0.003 ± 0.002	—	—
[13, 14]	0.037 ± 0.001 ± 0.003 ± 0.002	0.032 ± 0.001 ± 0.002 ± 0.002	0.029 ± 0.001 ± 0.002 ± 0.002	—	—

$d^2\sigma/(dp_T dy^*)$ [mb/(GeV/c)] (Backward)

p_T[GeV/c]\y^*	[−3, −2.5]	[−3.5, −3]	[−4, −3.5]	[−4.5, −4]	[−5, −4.5]
[1, 2]	20.016 ± 0.220 ± 0.866 ± 2.666	18.689 ± 0.079 ± 0.568 ± 2.120	17.293 ± 0.065 ± 0.508 ± 1.756	14.348 ± 0.206 ± 0.683 ± 1.395	10.639 ± 0.057 ± 0.815 ± 1.036
[2, 3]	12.676 ± 0.044 ± 0.377 ± 1.373	11.864 ± 0.022 ± 0.334 ± 1.214	10.054 ± 0.018 ± 0.233 ± 0.955	7.692 ± 0.020 ± 0.248 ± 0.678	5.165 ± 0.025 ± 0.526 ± 0.478
[3, 4]	5.957 ± 0.018 ± 0.154 ± 0.629	5.600 ± 0.010 ± 0.162 ± 0.530	4.519 ± 0.008 ± 0.138 ± 0.418	3.246 ± 0.010 ± 0.155 ± 0.284	2.046 ± 0.014 ± 0.150 ± 0.199
[4, 5]	2.788 ± 0.010 ± 0.091 ± 0.276	2.522 ± 0.006 ± 0.065 ± 0.230	1.996 ± 0.006 ± 0.104 ± 0.175	1.368 ± 0.005 ± 0.078 ± 0.121	0.766 ± 0.009 ± 0.077 ± 0.071
[5, 6]	1.356 ± 0.006 ± 0.042 ± 0.130	1.188 ± 0.002 ± 0.035 ± 0.105	0.912 ± 0.005 ± 0.039 ± 0.079	0.585 ± 0.003 ± 0.038 ± 0.054	0.298 ± 0.006 ± 0.029 ± 0.029
[6, 7]	0.687 ± 0.007 ± 0.016 ± 0.065	0.593 ± 0.001 ± 0.020 ± 0.053	0.428 ± 0.001 ± 0.018 ± 0.037	0.277 ± 0.002 ± 0.020 ± 0.027	0.117 ± 0.004 ± 0.015 ± 0.014
[7, 8]	0.382 ± 0.009 ± 0.012 ± 0.035	0.314 ± 0.002 ± 0.010 ± 0.029	0.226 ± 0.001 ± 0.012 ± 0.020	0.125 ± 0.002 ± 0.011 ± 0.014	0.068 ± 0.007 ± 0.014 ± 0.009
[8, 9]	0.214 ± 0.002 ± 0.007 ± 0.020	0.175 ± 0.001 ± 0.006 ± 0.016	0.118 ± 0.001 ± 0.005 ± 0.012	0.071 ± 0.002 ± 0.007 ± 0.008	—
[9, 10]	0.130 ± 0.001 ± 0.005 ± 0.013	0.102 ± 0.001 ± 0.004 ± 0.009	0.067 ± 0.001 ± 0.004 ± 0.006	0.033 ± 0.001 ± 0.005 ± 0.003	—
[10, 11]	0.081 ± 0.001 ± 0.004 ± 0.008	0.062 ± 0.001 ± 0.003 ± 0.006	0.041 ± 0.001 ± 0.003 ± 0.004	0.018 ± 0.001 ± 0.003 ± 0.002	—
[11, 12]	0.053 ± 0.001 ± 0.003 ± 0.005	0.040 ± 0.001 ± 0.002 ± 0.004	0.024 ± 0.001 ± 0.002 ± 0.002	0.022 ± 0.002 ± 0.005 ± 0.003	—
[12, 13]	0.035 ± 0.001 ± 0.002 ± 0.003	0.026 ± 0.000 ± 0.002 ± 0.002	0.015 ± 0.000 ± 0.001 ± 0.002	—	—
[13, 14]	0.023 ± 0.000 ± 0.001 ± 0.002	0.017 ± 0.000 ± 0.001 ± 0.002	0.010 ± 0.000 ± 0.001 ± 0.001	—	—

Table 4: Differential cross-section for prompt D_s^+ production as a function of p_{T} in pPb collisions at forward and backward rapidities. The first uncertainty is statistical, the second the component of the systematic uncertainty that is uncorrelated between bins and the third the correlated systematic component.

$p_{\mathrm{T}}[\,\mathrm{GeV}/c]$	$\mathrm{d}\sigma/\mathrm{d}p_{\mathrm{T}}\,[\,\mathrm{mb}/(\,\mathrm{GeV}/c)]$ (Forward)
$[1,2]$	$17.826 \pm 0.433 \pm 0.955 \pm 1.808$
$[2,3]$	$12.218 \pm 0.104 \pm 0.216 \pm 1.177$
$[3,4]$	$6.259 \pm 0.072 \pm 0.074 \pm 0.591$
$[4,5]$	$3.051 \pm 0.027 \pm 0.025 \pm 0.283$
$[5,6]$	$1.576 \pm 0.017 \pm 0.017 \pm 0.146$
$[6,7]$	$0.843 \pm 0.012 \pm 0.019 \pm 0.079$
$[7,8]$	$0.476 \pm 0.011 \pm 0.010 \pm 0.045$
$[8,9]$	$0.244 \pm 0.006 \pm 0.009 \pm 0.023$
$[9,10]$	$0.147 \pm 0.005 \pm 0.004 \pm 0.014$
$[10,11]$	$0.095 \pm 0.003 \pm 0.005 \pm 0.009$
$[11,12]$	$0.059 \pm 0.002 \pm 0.002 \pm 0.006$
$[12,13]$	$0.034 \pm 0.002 \pm 0.001 \pm 0.003$

$p_{\mathrm{T}}[\,\mathrm{GeV}/c]$	$\mathrm{d}\sigma/\mathrm{d}p_{\mathrm{T}}\,[\,\mathrm{mb}/(\,\mathrm{GeV}/c)]$ (Backward)
$[1,2]$	$20.196 \pm 0.421 \pm 0.975 \pm 2.700$
$[2,3]$	$12.163 \pm 0.119 \pm 0.196 \pm 1.490$
$[3,4]$	$5.729 \pm 0.050 \pm 0.073 \pm 0.694$
$[4,5]$	$2.553 \pm 0.025 \pm 0.029 \pm 0.300$
$[5,6]$	$1.182 \pm 0.014 \pm 0.020 \pm 0.143$
$[6,7]$	$0.524 \pm 0.009 \pm 0.012 \pm 0.063$
$[7,8]$	$0.276 \pm 0.004 \pm 0.005 \pm 0.031$
$[8,9]$	$0.153 \pm 0.004 \pm 0.004 \pm 0.018$
$[9,10]$	$0.083 \pm 0.002 \pm 0.003 \pm 0.011$
$[10,11]$	$0.053 \pm 0.002 \pm 0.003 \pm 0.007$
$[11,12]$	$0.029 \pm 0.001 \pm 0.001 \pm 0.003$
$[12,13]$	$0.019 \pm 0.001 \pm 0.001 \pm 0.002$

Table 5: Differential cross-section for prompt D^+ production as a function of p_T in pPb collisions at forward and backward rapidities. The first uncertainty is statistical, the second the component of the systematic uncertainty that is uncorrelated between bins and the third the correlated systematic component.

$p_T[\,\mathrm{GeV}/c]$	$\mathrm{d}\sigma/\mathrm{d}p_T\ [\mathrm{mb}/(\,\mathrm{GeV}/c)]$ (Forward)
$[1,2]$	$40.198 \pm 0.174 \pm 0.717 \pm 2.291$
$[2,3]$	$25.763 \pm 0.057 \pm 0.456 \pm 1.326$
$[3,4]$	$12.959 \pm 0.019 \pm 0.219 \pm 0.638$
$[4,5]$	$6.311 \pm 0.012 \pm 0.135 \pm 0.300$
$[5,6]$	$3.188 \pm 0.007 \pm 0.064 \pm 0.151$
$[6,7]$	$1.693 \pm 0.012 \pm 0.042 \pm 0.081$
$[7,8]$	$0.943 \pm 0.005 \pm 0.022 \pm 0.045$
$[8,9]$	$0.559 \pm 0.005 \pm 0.014 \pm 0.028$
$[9,10]$	$0.306 \pm 0.001 \pm 0.008 \pm 0.015$
$[10,11]$	$0.194 \pm 0.002 \pm 0.004 \pm 0.010$
$[11,12]$	$0.130 \pm 0.001 \pm 0.004 \pm 0.007$
$[12,13]$	$0.071 \pm 0.001 \pm 0.002 \pm 0.004$
$[13,14]$	$0.048 \pm 0.001 \pm 0.002 \pm 0.003$

$p_T[\,\mathrm{GeV}/c]$	$\mathrm{d}\sigma/\mathrm{d}p_T\ [\mathrm{mb}/(\,\mathrm{GeV}/c)]$ (Backward)
$[1,2]$	$40.492 \pm 0.161 \pm 0.785 \pm 4.317$
$[2,3]$	$23.726 \pm 0.031 \pm 0.402 \pm 2.241$
$[3,4]$	$10.684 \pm 0.014 \pm 0.170 \pm 0.981$
$[4,5]$	$4.720 \pm 0.008 \pm 0.094 \pm 0.414$
$[5,6]$	$2.170 \pm 0.005 \pm 0.041 \pm 0.188$
$[6,7]$	$1.050 \pm 0.004 \pm 0.020 \pm 0.093$
$[7,8]$	$0.557 \pm 0.006 \pm 0.013 \pm 0.051$
$[8,9]$	$0.289 \pm 0.002 \pm 0.007 \pm 0.026$
$[9,10]$	$0.166 \pm 0.001 \pm 0.004 \pm 0.015$
$[10,11]$	$0.101 \pm 0.001 \pm 0.003 \pm 0.010$
$[11,12]$	$0.069 \pm 0.001 \pm 0.003 \pm 0.007$
$[12,13]$	$0.038 \pm 0.000 \pm 0.002 \pm 0.003$
$[13,14]$	$0.025 \pm 0.000 \pm 0.001 \pm 0.002$

Table 6: Differential cross-section for prompt D_s^+ production as a function of y^* in pPb collisions at forward and backward rapidities. The first uncertainty is statistical, the second the component of the systematic uncertainty that is uncorrelated between bins and the third the correlated systematic component.

y^*	$\mathrm{d}\sigma/\mathrm{d}y^*$ [mb] (Forward)
$[1.5, 2.0]$	$19.032 \pm 0.467 \pm 1.622 \pm 2.098$
$[2.0, 2.5]$	$19.347 \pm 0.231 \pm 0.790 \pm 1.854$
$[2.5, 3.0]$	$18.918 \pm 0.276 \pm 0.482 \pm 1.749$
$[3.0, 3.5]$	$17.129 \pm 0.344 \pm 0.449 \pm 1.606$
$[3.5, 4.0]$	$11.227 \pm 0.594 \pm 0.414 \pm 1.113$

y^*	$\mathrm{d}\sigma/\mathrm{d}y^*$ [mb] (Backward)
$[-2.5, -3.0]$	$22.148 \pm 0.434 \pm 1.383 \pm 3.142$
$[-3.0, -3.5]$	$21.695 \pm 0.392 \pm 0.539 \pm 2.667$
$[-3.5, -4.0]$	$18.086 \pm 0.342 \pm 0.414 \pm 2.214$
$[-4.0, -4.5]$	$15.176 \pm 0.329 \pm 0.714 \pm 1.962$
$[-4.5, -5.0]$	$8.814 \pm 0.459 \pm 1.047 \pm 1.002$

Table 7: Differential cross-section for prompt D^+ production as a function of y^* in pPb collisions at forward and backward rapidities. The first uncertainty is statistical, the second the component of the systematic uncertainty that is uncorrelated between bins and the third the correlated systematic component.

y^*	$\mathrm{d}\sigma/\mathrm{d}y^*$ [mb] (Forward)
$[1.5, 2.0]$	$43.77 \pm 0.31 \pm 0.98 \pm 2.90$
$[2.0, 2.5]$	$43.18 \pm 0.10 \pm 0.71 \pm 2.26$
$[2.5, 3.0]$	$39.59 \pm 0.09 \pm 0.74 \pm 1.88$
$[3.0, 3.5]$	$33.58 \pm 0.09 \pm 0.58 \pm 1.62$
$[3.5, 4.0]$	$24.60 \pm 0.12 \pm 0.92 \pm 1.22$

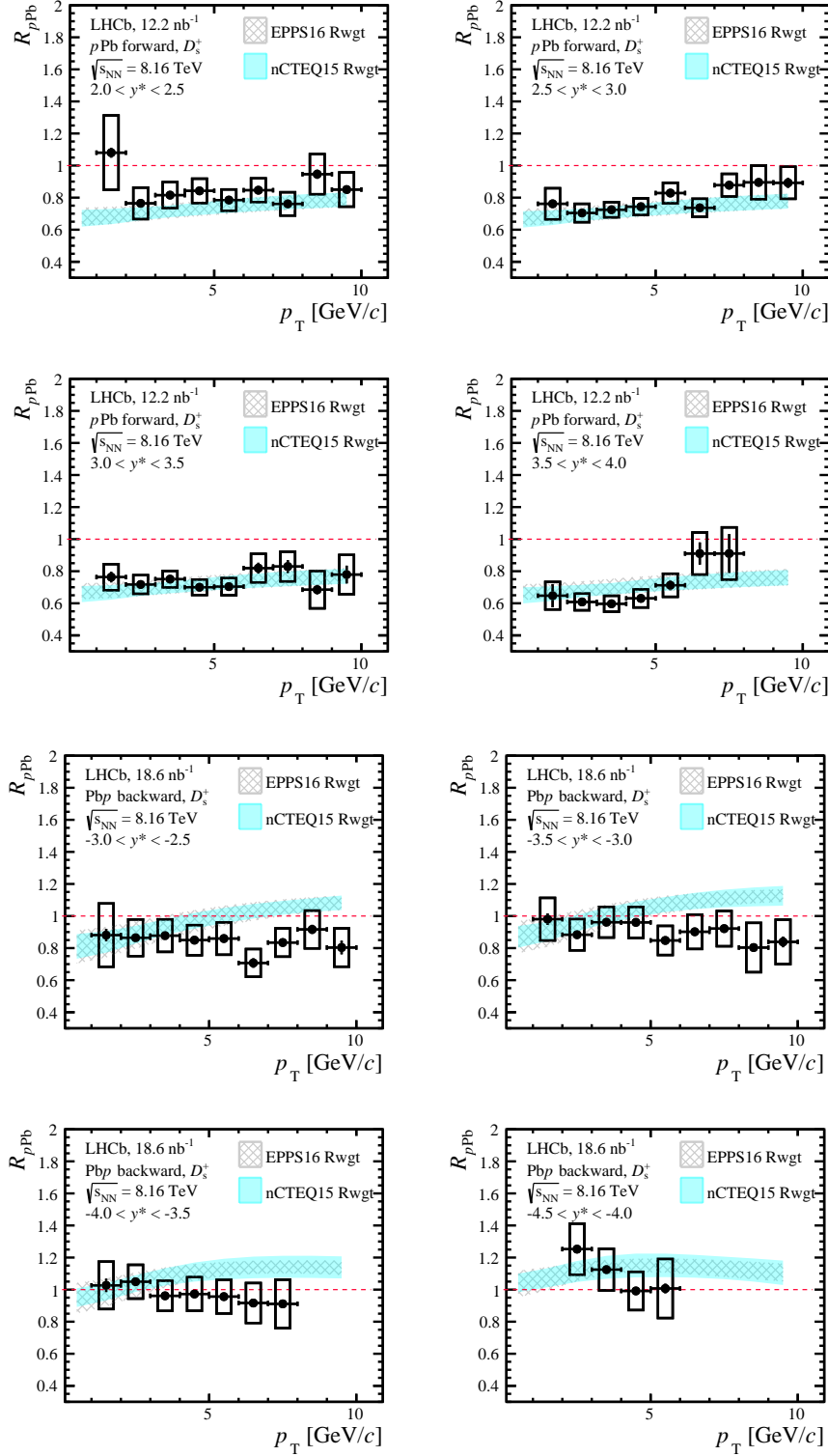| y^*	$\mathrm{d}\sigma/\mathrm{d}y^*$ [mb] (Backward)
$[-3.0, -2.5]$	$44.40 \pm 0.23 \pm 0.96 \pm 4.73$
$[-3.5, -3.0]$	$41.19 \pm 0.08 \pm 0.68 \pm 3.80$
$[-4.0, -3.5]$	$35.70 \pm 0.07 \pm 0.59 \pm 3.47$
$[-4.5, -4.0]$	$27.78 \pm 0.21 \pm 0.75 \pm 2.74$
$[-5.0, -4.5]$	$19.10 \pm 0.06 \pm 0.99 \pm 2.13$

Figure 13: Nuclear modification factor $R_{p\mathrm{Pb}}$ for prompt D_s^+ production as a function of p_T in different y^* intervals. The vertical error bars show the statistical uncertainties and the boxes show the systematic uncertainties. The coloured bands represent the theoretical calculations using the HELAC-Onia generator [49,50], incorporating nPDFs EPPS16 (grey) [52] and nCTEQ15 (blue) [53].
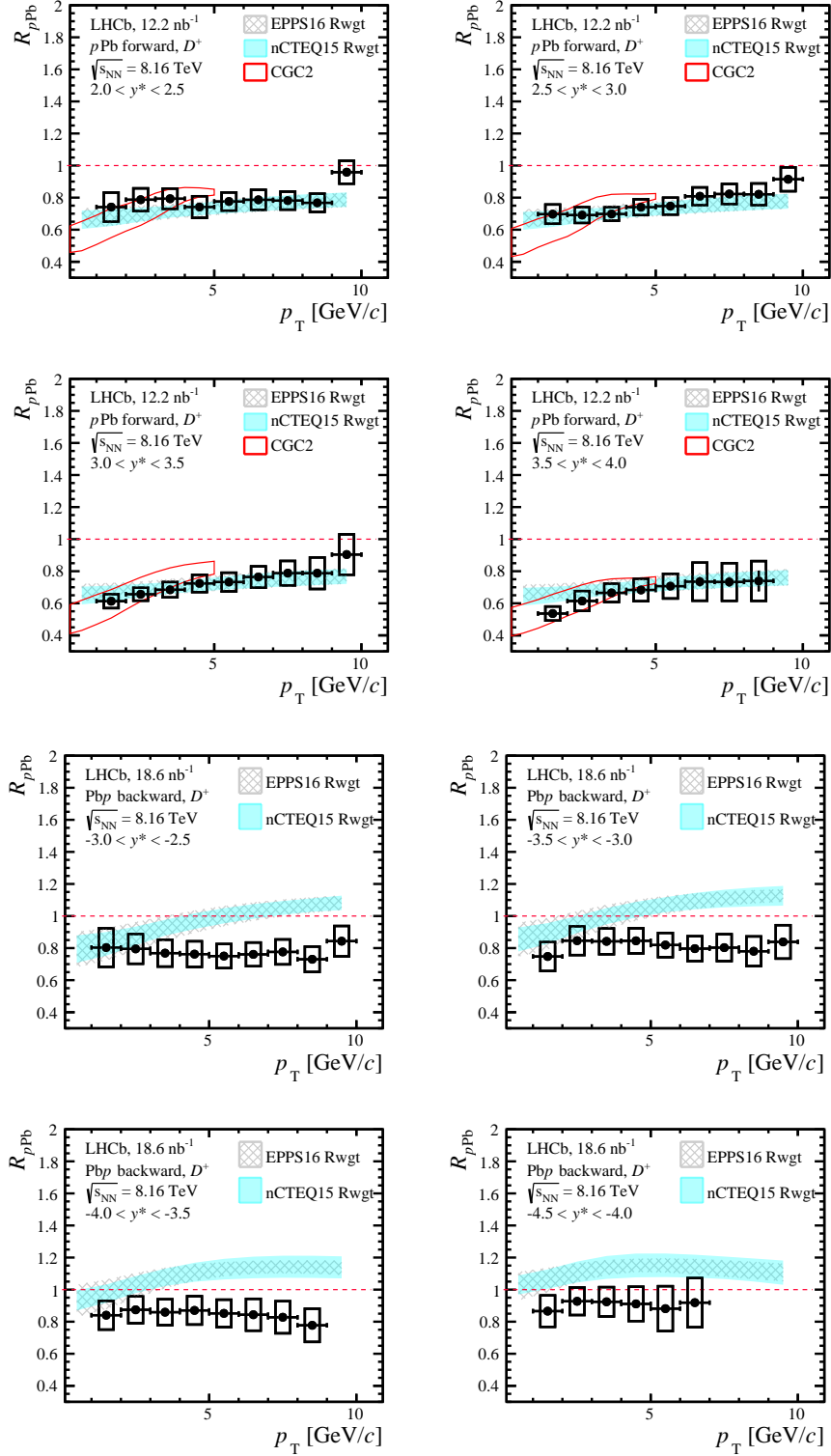
Figure 14: Nuclear modification factor $R_{p\text{Pb}}$ for prompt D^+ production as a function of p_T in different y^* intervals. The vertical error bars show the statistical uncertainties and the boxes show the systematic uncertainties. The coloured bands represent the theoretical calculations using the HELAC-Onia generator [49, 50], incorporating nPDFs EPPS16 (grey) [52] and nCTEQ15 (blue) [53]. The coloured line represent the CGC2 (red) calculations [61].
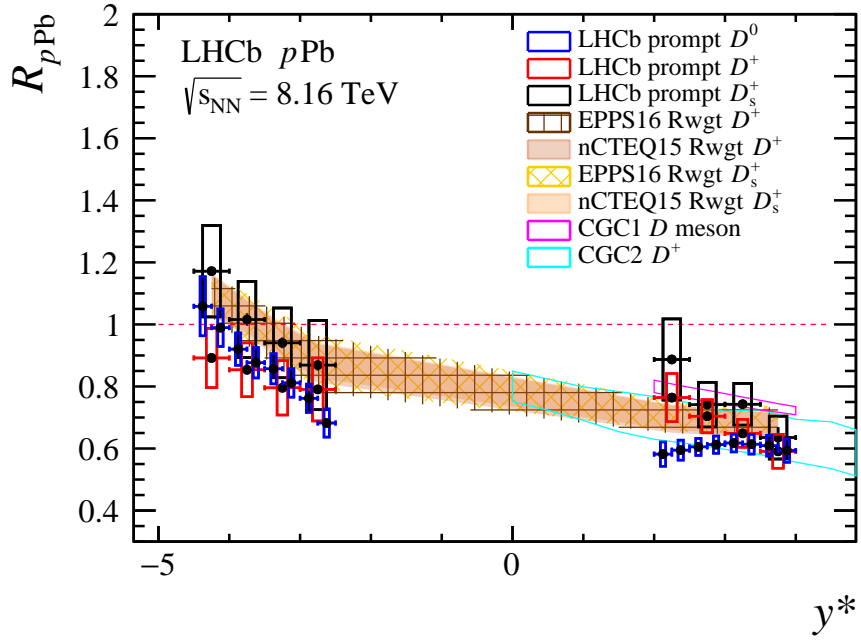
20

Figure 15: Nuclear modification factor as a function of y^* for prompt D^+ and D_s^+ mesons integrated over $1 < p_T < 10\,\mathrm{GeV}/c$. The vertical error bars show the statistical uncertainties and the boxes show the systematic uncertainties. The LHCb D^0 results at $\sqrt{s_{NN}} = 8.16$ TeV [7] and theoretical calculations at $\sqrt{s_{NN}} = 8.16$ TeV are also shown [52, 53, 59–61].

Table 8: Nuclear modification factor $R_{p\mathrm{Pb}}$ for prompt D_s^+ production as a function of p_{T} at forward (integrated over the common rapidity region of $2.0 < y^* < 4.0$) and backward (integrated over the common rapidity region of $-4.5 < y^* < -2.5$) rapidity. The first uncertainty is statistical, the second systematic.

$p_{\mathrm{T}}\,[\,\mathrm{GeV}/c\,]$	$R_{p\mathrm{Pb}}$ (Forward)
$[1,2]$	$0.800 \pm 0.021 \pm 0.112$
$[2,3]$	$0.705 \pm 0.005 \pm 0.066$
$[3,4]$	$0.731 \pm 0.006 \pm 0.057$
$[4,5]$	$0.742 \pm 0.007 \pm 0.058$
$[5,6]$	$0.764 \pm 0.008 \pm 0.063$
$[6,7]$	$0.816 \pm 0.014 \pm 0.080$
$[7,8]$	$0.829 \pm 0.022 \pm 0.090$
$[8,9]$	$0.852 \pm 0.016 \pm 0.117$
$[9,10]$	$0.845 \pm 0.019 \pm 0.109$
$p_{\mathrm{T}}\,[\,\mathrm{GeV}/c\,]$	$R_{p\mathrm{Pb}}$ (Backward)
$[1,2]$	$0.957 \pm 0.022 \pm 0.160$
$[2,3]$	$0.967 \pm 0.009 \pm 0.111$
$[3,4]$	$0.956 \pm 0.008 \pm 0.101$
$[4,5]$	$0.928 \pm 0.009 \pm 0.099$
$[5,6]$	$0.896 \pm 0.010 \pm 0.107$
$[6,7]$	$0.817 \pm 0.015 \pm 0.100$
$[7,8]$	$0.883 \pm 0.013 \pm 0.110$
$[8,9]$	$0.862 \pm 0.018 \pm 0.136$
$[9,10]$	$0.819 \pm 0.028 \pm 0.127$

Table 9: Nuclear modification factor $R_{p\mathrm{Pb}}$ for prompt D_s^+ production as a function of y^*, integrated over $1 < p_{\mathrm{T}} < 10\,\mathrm{GeV}/c$. The first uncertainty is statistical, the second systematic.

y^*	$R_{p\mathrm{Pb}}$
$[-4.5,-4.0]$	$1.172 \pm 0.012 \pm 0.147$
$[-4.0,-3.5]$	$1.016 \pm 0.019 \pm 0.123$
$[-3.5,-3.0]$	$0.941 \pm 0.017 \pm 0.112$
$[-3.0,-2.5]$	$0.869 \pm 0.017 \pm 0.144$
$[2.0,2.5]$	$0.887 \pm 0.011 \pm 0.131$
$[2.5,3.0]$	$0.742 \pm 0.011 \pm 0.072$
$[3.0,3.5]$	$0.743 \pm 0.015 \pm 0.067$
$[3.5,4.0]$	$0.635 \pm 0.034 \pm 0.069$

Table 10: Nuclear modification factor $R_{p\mathrm{Pb}}$ for prompt D_s^+ production as a function of p_T and y^*. The first uncertainty is statistical, the second systematic.

$R_{p\mathrm{Pb}}$ (Forward)

$p_\mathrm{T}[\mathrm{GeV}/c]\backslash y^*$	[2, 2.5]	[2.5, 3]	[3, 3.5]	[3.5, 4]
[1, 2]	$1.080 \pm 0.031 \pm 0.232$	$0.762 \pm 0.026 \pm 0.097$	$0.763 \pm 0.033 \pm 0.081$	$0.647 \pm 0.073 \pm 0.086$
[2, 3]	$0.764 \pm 0.007 \pm 0.098$	$0.704 \pm 0.006 \pm 0.057$	$0.717 \pm 0.011 \pm 0.058$	$0.608 \pm 0.018 \pm 0.052$
[3, 4]	$0.816 \pm 0.012 \pm 0.081$	$0.724 \pm 0.007 \pm 0.047$	$0.750 \pm 0.010 \pm 0.051$	$0.597 \pm 0.022 \pm 0.050$
[4, 5]	$0.842 \pm 0.011 \pm 0.076$	$0.743 \pm 0.008 \pm 0.052$	$0.700 \pm 0.017 \pm 0.048$	$0.630 \pm 0.025 \pm 0.056$
[5, 6]	$0.785 \pm 0.015 \pm 0.067$	$0.828 \pm 0.012 \pm 0.064$	$0.704 \pm 0.014 \pm 0.053$	$0.713 \pm 0.031 \pm 0.072$
[6, 7]	$0.846 \pm 0.010 \pm 0.074$	$0.737 \pm 0.013 \pm 0.056$	$0.819 \pm 0.034 \pm 0.089$	$0.910 \pm 0.069 \pm 0.131$
[7, 8]	$0.761 \pm 0.014 \pm 0.073$	$0.877 \pm 0.021 \pm 0.071$	$0.829 \pm 0.040 \pm 0.093$	$0.911 \pm 0.121 \pm 0.163$
[8, 9]	$0.946 \pm 0.029 \pm 0.125$	$0.895 \pm 0.022 \pm 0.105$	$0.685 \pm 0.030 \pm 0.116$	–
[9, 10]	$0.850 \pm 0.019 \pm 0.107$	$0.893 \pm 0.031 \pm 0.100$	$0.779 \pm 0.055 \pm 0.122$	–

$R_{p\mathrm{Pb}}$ (Backward)

$p_\mathrm{T}[\mathrm{GeV}/c]\backslash y^*$	[−3, −2.5]	[−3.5, −3]	[−4, −3.5]	[−4.5, −4]
[1, 2]	$0.881 \pm 0.039 \pm 0.197$	$0.980 \pm 0.035 \pm 0.133$	$1.026 \pm 0.042 \pm 0.148$	–
[2, 3]	$0.865 \pm 0.017 \pm 0.114$	$0.883 \pm 0.020 \pm 0.097$	$1.049 \pm 0.011 \pm 0.105$	$1.252 \pm 0.020 \pm 0.159$
[3, 4]	$0.878 \pm 0.009 \pm 0.102$	$0.961 \pm 0.023 \pm 0.096$	$0.961 \pm 0.017 \pm 0.094$	$1.125 \pm 0.016 \pm 0.130$
[4, 5]	$0.849 \pm 0.020 \pm 0.094$	$0.960 \pm 0.011 \pm 0.097$	$0.973 \pm 0.021 \pm 0.105$	$0.992 \pm 0.012 \pm 0.120$
[5, 6]	$0.860 \pm 0.026 \pm 0.101$	$0.848 \pm 0.010 \pm 0.091$	$0.956 \pm 0.012 \pm 0.105$	$1.007 \pm 0.030 \pm 0.184$
[6, 7]	$0.707 \pm 0.030 \pm 0.087$	$0.902 \pm 0.012 \pm 0.107$	$0.916 \pm 0.020 \pm 0.124$	–
[7, 8]	$0.835 \pm 0.022 \pm 0.088$	$0.921 \pm 0.023 \pm 0.110$	$0.911 \pm 0.021 \pm 0.151$	–
[8, 9]	$0.916 \pm 0.029 \pm 0.118$	$0.803 \pm 0.020 \pm 0.154$	–	–
[9, 10]	$0.804 \pm 0.042 \pm 0.119$	$0.839 \pm 0.033 \pm 0.139$	–	–

Table 11: Nuclear modification factor $R_{p\mathrm{Pb}}$ for prompt D^+ production as a function of p_{T} at forward (integrated over the common rapidity region of $2.0 < y^* < 4.0$) and backward (integrated over the common rapidity region of $-4.5 < y^* < -2.5$) rapidity. The first uncertainty is statistical, the second systematic.

$p_{\mathrm{T}}\ [\,\mathrm{GeV}/c\,]$	$R_{p\mathrm{Pb}}$ (Forward)
$[1, 2]$	$0.652 \pm 0.002 \pm 0.058$
$[2, 3]$	$0.693 \pm 0.002 \pm 0.053$
$[3, 4]$	$0.715 \pm 0.001 \pm 0.051$
$[4, 5]$	$0.727 \pm 0.001 \pm 0.059$
$[5, 6]$	$0.746 \pm 0.002 \pm 0.058$
$[6, 7]$	$0.779 \pm 0.005 \pm 0.070$
$[7, 8]$	$0.787 \pm 0.005 \pm 0.071$
$[8, 9]$	$0.783 \pm 0.010 \pm 0.078$
$[9, 10]$	$0.929 \pm 0.006 \pm 0.087$
$p_{\mathrm{T}}\ [\,\mathrm{GeV}/c\,]$	$R_{p\mathrm{Pb}}$ (Backward)
$[1, 2]$	$0.808 \pm 0.004 \pm 0.100$
$[2, 3]$	$0.850 \pm 0.001 \pm 0.089$
$[3, 4]$	$0.834 \pm 0.001 \pm 0.083$
$[4, 5]$	$0.831 \pm 0.001 \pm 0.085$
$[5, 6]$	$0.809 \pm 0.002 \pm 0.085$
$[6, 7]$	$0.808 \pm 0.003 \pm 0.088$
$[7, 8]$	$0.797 \pm 0.008 \pm 0.085$
$[8, 9]$	$0.758 \pm 0.004 \pm 0.089$
$[9, 10]$	$0.841 \pm 0.005 \pm 0.098$

Table 12: Nuclear modification factor $R_{p\mathrm{Pb}}$ for prompt D^+ production as a function of y^*, integrated over $1 < p_{\mathrm{T}} < 10\,\mathrm{GeV}/c$. The first uncertainty is statistical, the second systematic.

y^*	$R_{p\mathrm{Pb}}$
$[-4.5, -4.0]$	$0.892 \pm 0.007 \pm 0.096$
$[-4.0, -3.5]$	$0.854 \pm 0.002 \pm 0.087$
$[-3.5, -3.0]$	$0.796 \pm 0.002 \pm 0.088$
$[-3.0, -2.5]$	$0.791 \pm 0.004 \pm 0.102$
$[2.0, 2.5]$	$0.764 \pm 0.002 \pm 0.078$
$[2.5, 3.0]$	$0.704 \pm 0.002 \pm 0.053$
$[3.0, 3.5]$	$0.649 \pm 0.002 \pm 0.045$
$[3.5, 4.0]$	$0.591 \pm 0.003 \pm 0.055$

Table 13: Nuclear modification factor $R_{p\mathrm{Pb}}$ for prompt D^+ production as a function of p_T and y^*. The first uncertainty is statistical, the second systematic.

$R_{p\mathrm{Pb}}$ (Forward)

$p_\mathrm{T}[\mathrm{GeV}/c]\backslash y^*$	[2, 2.5]	[2.5, 3]	[3, 3.5]	[3.5, 4]
[1, 2]	$0.741 \pm 0.004 \pm 0.091$	$0.697 \pm 0.001 \pm 0.060$	$0.613 \pm 0.003 \pm 0.044$	$0.536 \pm 0.005 \pm 0.044$
[2, 3]	$0.787 \pm 0.002 \pm 0.071$	$0.691 \pm 0.005 \pm 0.049$	$0.657 \pm 0.002 \pm 0.040$	$0.614 \pm 0.003 \pm 0.062$
[3, 4]	$0.793 \pm 0.002 \pm 0.063$	$0.698 \pm 0.001 \pm 0.042$	$0.684 \pm 0.002 \pm 0.048$	$0.665 \pm 0.004 \pm 0.057$
[4, 5]	$0.742 \pm 0.001 \pm 0.067$	$0.740 \pm 0.002 \pm 0.050$	$0.724 \pm 0.003 \pm 0.054$	$0.683 \pm 0.006 \pm 0.070$
[5, 6]	$0.776 \pm 0.002 \pm 0.057$	$0.747 \pm 0.003 \pm 0.052$	$0.733 \pm 0.003 \pm 0.058$	$0.707 \pm 0.008 \pm 0.077$
[6, 7]	$0.786 \pm 0.004 \pm 0.062$	$0.808 \pm 0.005 \pm 0.055$	$0.764 \pm 0.005 \pm 0.066$	$0.735 \pm 0.029 \pm 0.119$
[7, 8]	$0.781 \pm 0.005 \pm 0.056$	$0.822 \pm 0.005 \pm 0.063$	$0.788 \pm 0.008 \pm 0.076$	$0.733 \pm 0.030 \pm 0.118$
[8, 9]	$0.768 \pm 0.005 \pm 0.057$	$0.821 \pm 0.006 \pm 0.068$	$0.788 \pm 0.011 \pm 0.098$	$0.739 \pm 0.065 \pm 0.124$
[9, 10]	$0.958 \pm 0.008 \pm 0.072$	$0.915 \pm 0.010 \pm 0.075$	$0.904 \pm 0.015 \pm 0.126$	–

$R_{p\mathrm{Pb}}$ (Backward)

$p_\mathrm{T}[\mathrm{GeV}/c]\backslash y^*$	[−3, −2.5]	[−3.5, −3]	[−4, −3.5]	[−4.5, −4]
[1, 2]	$0.803 \pm 0.009 \pm 0.120$	$0.748 \pm 0.003 \pm 0.091$	$0.840 \pm 0.003 \pm 0.090$	$0.866 \pm 0.012 \pm 0.098$
[2, 3]	$0.795 \pm 0.003 \pm 0.093$	$0.846 \pm 0.002 \pm 0.090$	$0.874 \pm 0.002 \pm 0.084$	$0.927 \pm 0.002 \pm 0.086$
[3, 4]	$0.769 \pm 0.002 \pm 0.084$	$0.842 \pm 0.001 \pm 0.081$	$0.859 \pm 0.002 \pm 0.081$	$0.924 \pm 0.003 \pm 0.092$
[4, 5]	$0.762 \pm 0.003 \pm 0.080$	$0.845 \pm 0.002 \pm 0.078$	$0.870 \pm 0.003 \pm 0.089$	$0.911 \pm 0.003 \pm 0.107$
[5, 6]	$0.750 \pm 0.003 \pm 0.075$	$0.819 \pm 0.002 \pm 0.076$	$0.852 \pm 0.005 \pm 0.086$	$0.881 \pm 0.004 \pm 0.140$
[6, 7]	$0.761 \pm 0.008 \pm 0.074$	$0.797 \pm 0.002 \pm 0.077$	$0.843 \pm 0.002 \pm 0.099$	$0.919 \pm 0.008 \pm 0.153$
[7, 8]	$0.776 \pm 0.018 \pm 0.078$	$0.803 \pm 0.006 \pm 0.084$	$0.827 \pm 0.005 \pm 0.100$	–
[8, 9]	$0.730 \pm 0.008 \pm 0.079$	$0.780 \pm 0.004 \pm 0.092$	$0.777 \pm 0.009 \pm 0.104$	–
[9, 10]	$0.843 \pm 0.005 \pm 0.095$	$0.839 \pm 0.009 \pm 0.104$	–	–

Table 14: Forward and backward production ratio R_{FB} for prompt D_s^+ mesons as a function of p_{T} and y^*. The first uncertainty is statistical, the second systematic.

$p_{\mathrm{T}}\,[\,\mathrm{GeV}/c\,]$	R_{FB}
$[1, 2]$	$0.763 \pm 0.032 \pm 0.103$
$[2, 3]$	$0.743 \pm 0.011 \pm 0.079$
$[3, 4]$	$0.752 \pm 0.011 \pm 0.075$
$[4, 5]$	$0.764 \pm 0.013 \pm 0.073$
$[5, 6]$	$0.858 \pm 0.016 \pm 0.084$
$[6, 7]$	$0.982 \pm 0.030 \pm 0.102$
$[7, 8]$	$0.980 \pm 0.030 \pm 0.089$
$[8, 9]$	$0.921 \pm 0.028 \pm 0.092$
$[9, 10]$	$1.028 \pm 0.051 \pm 0.119$
$[10, 11]$	$0.978 \pm 0.057 \pm 0.148$
$[11, 12]$	$1.028 \pm 0.074 \pm 0.144$
$[12, 13]$	$1.068 \pm 0.144 \pm 0.161$
$|y^*|$	R_{FB}
$[2.5, 3.0]$	$0.854 \pm 0.021 \pm 0.119$
$[3.0, 3.5]$	$0.790 \pm 0.021 \pm 0.084$
$[3.5, 4.0]$	$0.623 \pm 0.035 \pm 0.071$

Table 15: Forward and backward production ratio R_{FB} for prompt D^+ mesons as a function of p_{T} and y^*. The first uncertainty is statistical, the second systematic.

$p_{\mathrm{T}}\,[\,\mathrm{GeV}/c\,]$	R_{FB}
$[1, 2]$	$0.775 \pm 0.004 \pm 0.092$
$[2, 3]$	$0.785 \pm 0.003 \pm 0.082$
$[3, 4]$	$0.832 \pm 0.002 \pm 0.083$
$[4, 5]$	$0.878 \pm 0.003 \pm 0.086$
$[5, 6]$	$0.913 \pm 0.004 \pm 0.088$
$[6, 7]$	$0.979 \pm 0.010 \pm 0.097$
$[7, 8]$	$0.993 \pm 0.014 \pm 0.101$
$[8, 9]$	$1.048 \pm 0.022 \pm 0.111$
$[9, 10]$	$1.081 \pm 0.013 \pm 0.118$
$[10, 11]$	$1.103 \pm 0.022 \pm 0.127$
$[11, 12]$	$1.097 \pm 0.028 \pm 0.126$
$[12, 13]$	$1.101 \pm 0.049 \pm 0.137$
$[13, 14]$	$1.272 \pm 0.044 \pm 0.163$
$|y^*|$	R_{FB}
$[2.5, 3.0]$	$0.881 \pm 0.005 \pm 0.104$
$[3.0, 3.5]$	$0.814 \pm 0.003 \pm 0.086$
$[3.5, 4.0]$	$0.690 \pm 0.004 \pm 0.072$
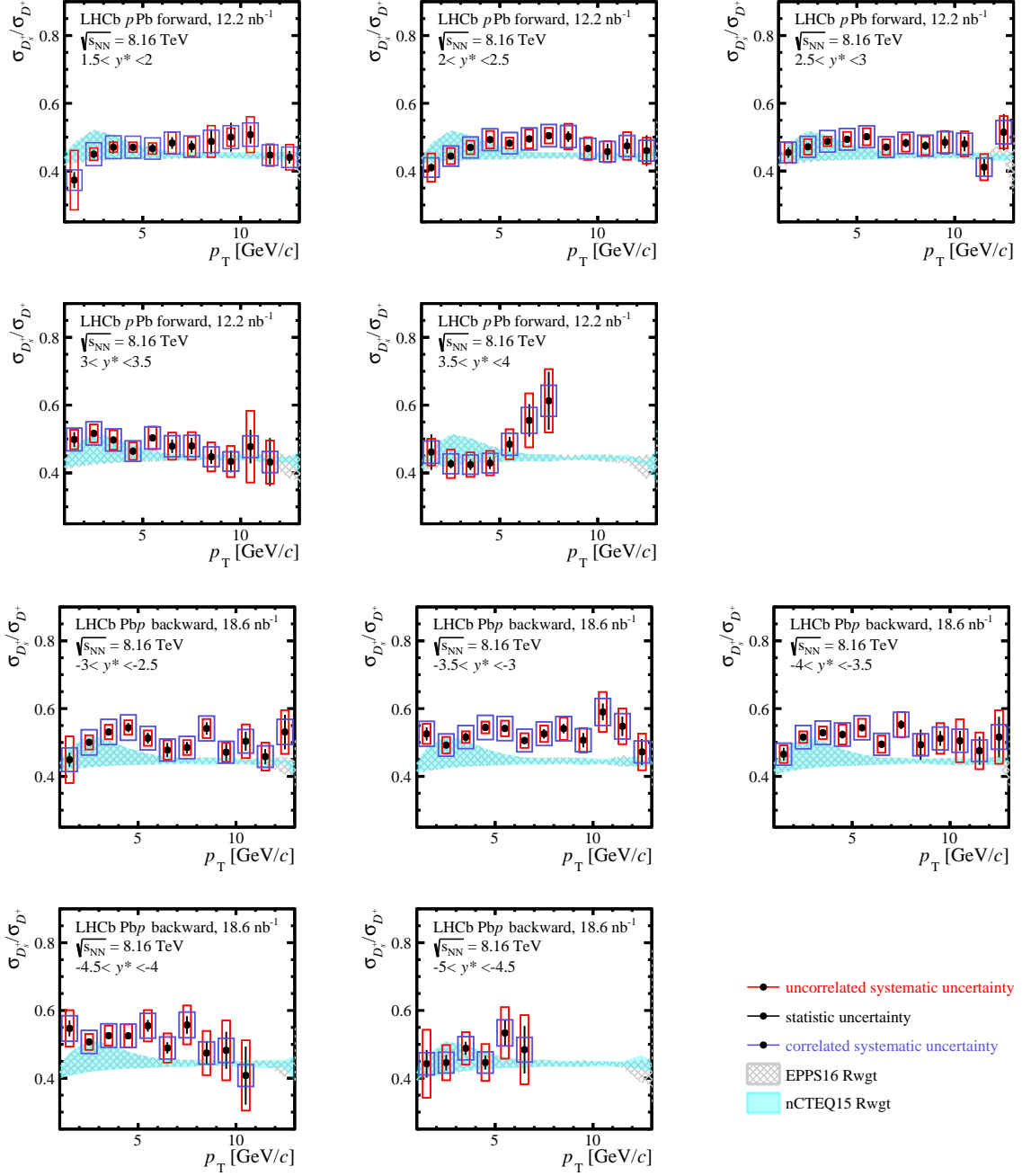
Figure 16: The production cross-section ratio $\sigma_{D_s^+}/\sigma_{D^+}$ as a function of p_{T} and y^* in pPb collisions. The error bars show the statistical uncertainty, the red boxes the uncorrelated systematic uncertainty and the blue boxes the correlated systematic uncertainty. The coloured bands correspond to the theoretical calculations, incorporating nPDFs EPPS16 (gray) [52] and nCTEQ15 (cyan) [53].

Table 16: The production cross-section ratio $\sigma_{D_s^+}/\sigma_{D^+}$ as a function of p_{T} and y^* in pPb collisions at (upper) forward and (lower) backward rapidities. The first uncertainty is statistical, the second the component of the systematic uncertainty that is uncorrelated between bins and the third the correlated systematic component.

$\sigma_{D_s^+}/\sigma_{D^+}$ (Forward)

$p_{\mathrm{T}}[\mathrm{GeV}/c]\backslash y^*$	[1.5, 2]	[2, 2.5]	[2.5, 3]	[3, 3.5]	[3.5, 4]
[1, 2]	$0.373 \pm 0.023 \pm 0.088 \pm 0.030$	$0.410 \pm 0.012 \pm 0.042 \pm 0.029$	$0.455 \pm 0.015 \pm 0.030 \pm 0.031$	$0.499 \pm 0.022 \pm 0.029 \pm 0.034$	$0.461 \pm 0.052 \pm 0.039 \pm 0.033$
[2, 3]	$0.450 \pm 0.013 \pm 0.018 \pm 0.034$	$0.444 \pm 0.004 \pm 0.024 \pm 0.030$	$0.472 \pm 0.006 \pm 0.023 \pm 0.031$	$0.516 \pm 0.008 \pm 0.027 \pm 0.034$	$0.427 \pm 0.013 \pm 0.042 \pm 0.029$
[3, 4]	$0.471 \pm 0.019 \pm 0.015 \pm 0.034$	$0.470 \pm 0.007 \pm 0.020 \pm 0.031$	$0.488 \pm 0.005 \pm 0.014 \pm 0.032$	$0.497 \pm 0.007 \pm 0.029 \pm 0.033$	$0.425 \pm 0.016 \pm 0.036 \pm 0.028$
[4, 5]	$0.470 \pm 0.009 \pm 0.015 \pm 0.032$	$0.493 \pm 0.007 \pm 0.026 \pm 0.032$	$0.494 \pm 0.006 \pm 0.022 \pm 0.032$	$0.464 \pm 0.011 \pm 0.026 \pm 0.030$	$0.429 \pm 0.018 \pm 0.036 \pm 0.029$
[5, 6]	$0.466 \pm 0.013 \pm 0.017 \pm 0.032$	$0.482 \pm 0.009 \pm 0.016 \pm 0.031$	$0.501 \pm 0.007 \pm 0.025 \pm 0.032$	$0.503 \pm 0.010 \pm 0.033 \pm 0.033$	$0.485 \pm 0.022 \pm 0.044 \pm 0.033$
[6, 7]	$0.483 \pm 0.017 \pm 0.032 \pm 0.033$	$0.495 \pm 0.006 \pm 0.028 \pm 0.032$	$0.471 \pm 0.009 \pm 0.023 \pm 0.030$	$0.479 \pm 0.020 \pm 0.040 \pm 0.031$	$0.555 \pm 0.048 \pm 0.080 \pm 0.038$
[7, 8]	$0.472 \pm 0.017 \pm 0.028 \pm 0.032$	$0.504 \pm 0.010 \pm 0.023 \pm 0.033$	$0.483 \pm 0.012 \pm 0.025 \pm 0.031$	$0.480 \pm 0.024 \pm 0.041 \pm 0.031$	$0.613 \pm 0.085 \pm 0.094 \pm 0.046$
[8, 9]	$0.487 \pm 0.036 \pm 0.047 \pm 0.033$	$0.502 \pm 0.016 \pm 0.038 \pm 0.033$	$0.475 \pm 0.012 \pm 0.027 \pm 0.031$	$0.447 \pm 0.020 \pm 0.043 \pm 0.029$	–
[9, 10]	$0.500 \pm 0.042 \pm 0.027 \pm 0.034$	$0.467 \pm 0.011 \pm 0.033 \pm 0.030$	$0.485 \pm 0.018 \pm 0.034 \pm 0.031$	$0.434 \pm 0.032 \pm 0.046 \pm 0.029$	–
[10, 11]	$0.508 \pm 0.026 \pm 0.053 \pm 0.035$	$0.457 \pm 0.023 \pm 0.031 \pm 0.030$	$0.480 \pm 0.022 \pm 0.037 \pm 0.031$	$0.478 \pm 0.049 \pm 0.106 \pm 0.032$	–
[11, 12]	$0.447 \pm 0.027 \pm 0.033 \pm 0.030$	$0.474 \pm 0.021 \pm 0.041 \pm 0.031$	$0.412 \pm 0.024 \pm 0.039 \pm 0.027$	$0.432 \pm 0.071 \pm 0.064 \pm 0.031$	–
[12, 13]	$0.441 \pm 0.019 \pm 0.037 \pm 0.030$	$0.460 \pm 0.045 \pm 0.038 \pm 0.030$	$0.514 \pm 0.053 \pm 0.048 \pm 0.034$	–	–

$\sigma_{D_s^+}/\sigma_{D^+}$ (Backward)

| $p_{\mathrm{T}}[\mathrm{GeV}/c]\backslash y^*$	[-3, -2.5]	[-3.5, -3]	[-4, -3.5]	[-4.5, -4]	[-5, -4.5]
[1, 2]	$0.449 \pm 0.020 \pm 0.069 \pm 0.035$	$0.525 \pm 0.019 \pm 0.030 \pm 0.037$	$0.465 \pm 0.019 \pm 0.026 \pm 0.033$	$0.547 \pm 0.023 \pm 0.054 \pm 0.038$	$0.443 \pm 0.040 \pm 0.100 \pm 0.033$
[2, 3]	$0.500 \pm 0.010 \pm 0.021 \pm 0.037$	$0.492 \pm 0.011 \pm 0.024 \pm 0.033$	$0.516 \pm 0.005 \pm 0.017 \pm 0.034$	$0.507 \pm 0.008 \pm 0.024 \pm 0.034$	$0.446 \pm 0.023 \pm 0.052 \pm 0.031$
[3, 4]	$0.531 \pm 0.005 \pm 0.021 \pm 0.037$	$0.516 \pm 0.012 \pm 0.017 \pm 0.034$	$0.529 \pm 0.009 \pm 0.019 \pm 0.035$	$0.526 \pm 0.007 \pm 0.030 \pm 0.035$	$0.488 \pm 0.019 \pm 0.048 \pm 0.034$
[4, 5]	$0.544 \pm 0.013 \pm 0.021 \pm 0.037$	$0.544 \pm 0.006 \pm 0.017 \pm 0.036$	$0.523 \pm 0.011 \pm 0.029 \pm 0.034$	$0.525 \pm 0.006 \pm 0.034 \pm 0.034$	$0.446 \pm 0.020 \pm 0.054 \pm 0.031$
[5, 6]	$0.513 \pm 0.015 \pm 0.023 \pm 0.035$	$0.541 \pm 0.007 \pm 0.023 \pm 0.036$	$0.543 \pm 0.008 \pm 0.026 \pm 0.035$	$0.555 \pm 0.017 \pm 0.046 \pm 0.036$	$0.534 \pm 0.038 \pm 0.076 \pm 0.038$
[6, 7]	$0.478 \pm 0.021 \pm 0.029 \pm 0.033$	$0.506 \pm 0.007 \pm 0.022 \pm 0.033$	$0.495 \pm 0.011 \pm 0.025 \pm 0.032$	$0.489 \pm 0.017 \pm 0.043 \pm 0.032$	$0.484 \pm 0.070 \pm 0.102 \pm 0.037$
[7, 8]	$0.485 \pm 0.017 \pm 0.022 \pm 0.033$	$0.526 \pm 0.014 \pm 0.024 \pm 0.035$	$0.553 \pm 0.013 \pm 0.037 \pm 0.036$	$0.557 \pm 0.026 \pm 0.057 \pm 0.038$	–
[8, 9]	$0.541 \pm 0.018 \pm 0.028 \pm 0.037$	$0.541 \pm 0.013 \pm 0.033 \pm 0.036$	$0.493 \pm 0.044 \pm 0.032 \pm 0.032$	$0.474 \pm 0.032 \pm 0.065 \pm 0.033$	–
[9, 10]	$0.471 \pm 0.025 \pm 0.028 \pm 0.032$	$0.507 \pm 0.021 \pm 0.036 \pm 0.034$	$0.512 \pm 0.021 \pm 0.045 \pm 0.034$	$0.482 \pm 0.055 \pm 0.088 \pm 0.036$	–
[10, 11]	$0.504 \pm 0.028 \pm 0.050 \pm 0.035$	$0.590 \pm 0.025 \pm 0.059 \pm 0.040$	$0.505 \pm 0.029 \pm 0.063 \pm 0.034$	$0.408 \pm 0.085 \pm 0.104 \pm 0.032$	–
[11, 12]	$0.458 \pm 0.022 \pm 0.041 \pm 0.032$	$0.548 \pm 0.028 \pm 0.053 \pm 0.037$	$0.475 \pm 0.041 \pm 0.054 \pm 0.032$	–	–
[12, 13]	$0.531 \pm 0.051 \pm 0.065 \pm 0.037$	$0.472 \pm 0.038 \pm 0.054 \pm 0.032$	$0.516 \pm 0.060 \pm 0.079 \pm 0.036$	–	–
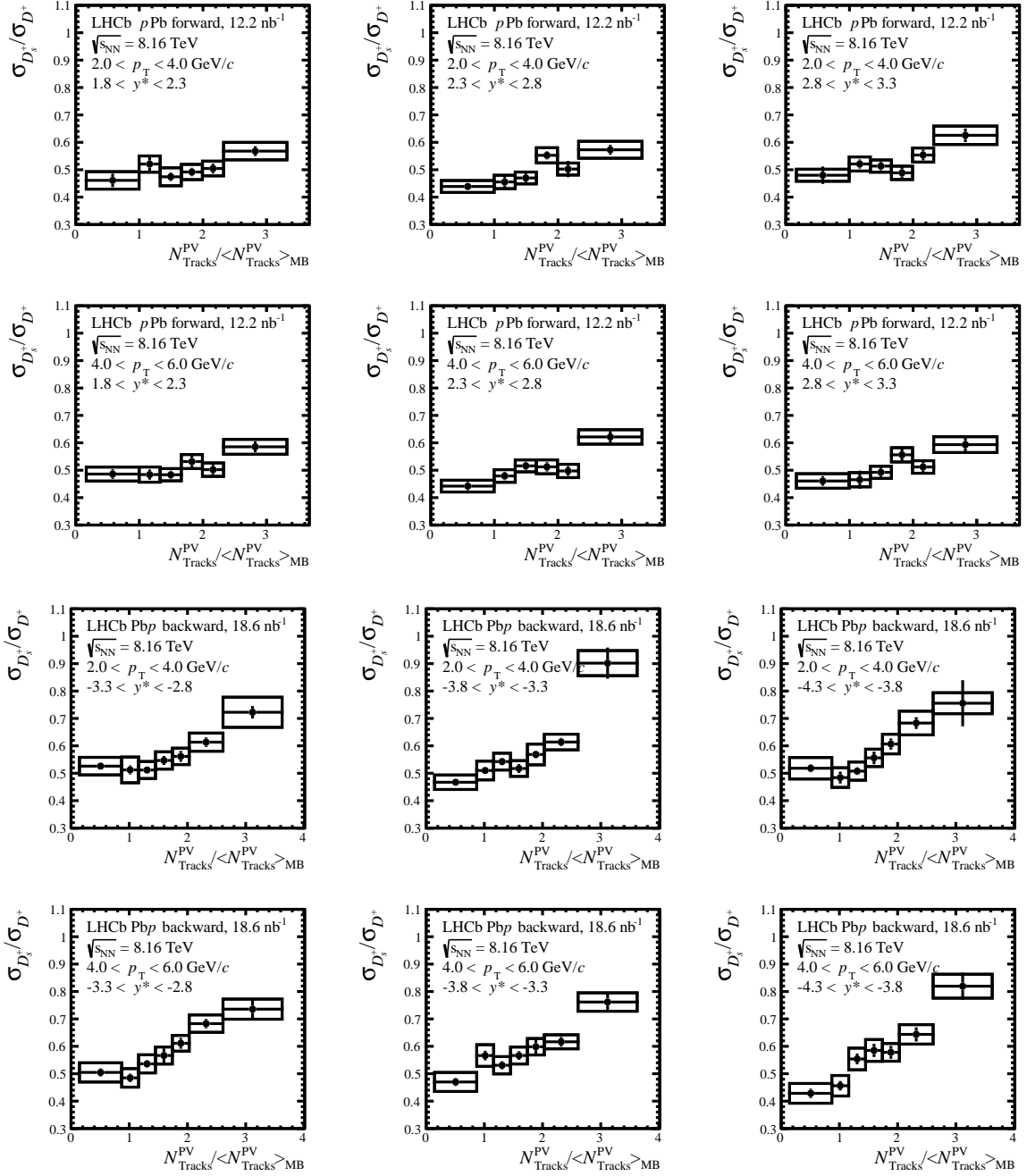
Figure 17: The production cross-section ratio, $\sigma_{D_s^+}/\sigma_{D^+}$, versus normalized event multiplicity in different D-meson p_{T} (2-6 GeV/c) and y^* ranges for the (six upper plots) forward and (six lower plots) backward rapidities. The vertical error bars show the statistical uncertainty, the boxes the systematic.
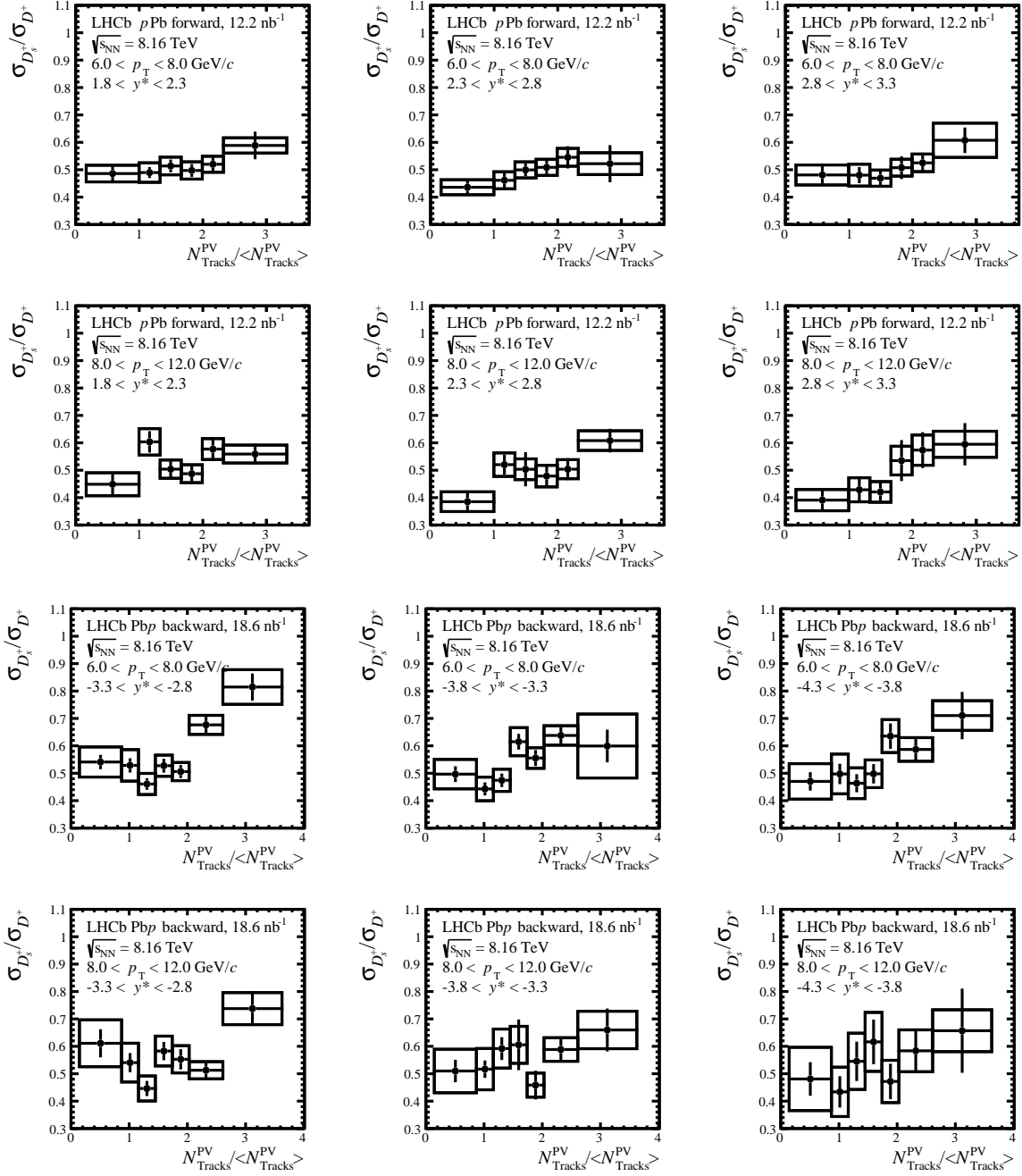
Figure 18: The production cross-section ratio, $\sigma_{D_s^+}/\sigma_{D^+}$, versus normalized event multiplicity in different D-meson p_T (6-12 GeV/c) and y^* ranges for the (six upper plots) forward and (six lower plots) backward rapidities. The vertical error bars show the statistical uncertainty, the boxes the systematic.

Table 17: The production cross-section ratio $\sigma_{D_s^+}/\sigma_{D^+}$ as a function of p_T, y^* and $N_{\text{Tracks}}^{\text{PV}}$ in pPb collisions at (upper) forward and (lower) backward rapidities. The first uncertainty is statistical, the second the component of the systematic uncertainty that is uncorrelated between bins and the third the correlated systematic component.

$\sigma_{D_s^+}/\sigma_{D^+}$ (Forward)

p_T [GeV/c], y^* \ $N_{\text{tracks}}^{\text{PV}}$	[10, 60]	[60, 80]	[80, 100]	[100, 120]	[120, 140]	[140, 200]
[2, 4], [1.8, 2.3]	$0.46 \pm 0.02 \pm 0.02 \pm 0.02$	$0.52 \pm 0.03 \pm 0.02 \pm 0.02$	$0.47 \pm 0.02 \pm 0.03 \pm 0.02$	$0.49 \pm 0.02 \pm 0.02 \pm 0.02$	$0.50 \pm 0.02 \pm 0.02 \pm 0.02$	$0.57 \pm 0.02 \pm 0.02 \pm 0.03$
[2, 4], [2.3, 2.8]	$0.44 \pm 0.01 \pm 0.01 \pm 0.02$	$0.46 \pm 0.02 \pm 0.02 \pm 0.02$	$0.47 \pm 0.02 \pm 0.02 \pm 0.01$	$0.55 \pm 0.01 \pm 0.02 \pm 0.02$	$0.50 \pm 0.03 \pm 0.02 \pm 0.02$	$0.57 \pm 0.02 \pm 0.02 \pm 0.02$
[2, 4], [2.8, 3.3]	$0.48 \pm 0.03 \pm 0.02 \pm 0.02$	$0.52 \pm 0.02 \pm 0.02 \pm 0.02$	$0.51 \pm 0.02 \pm 0.02 \pm 0.02$	$0.49 \pm 0.02 \pm 0.02 \pm 0.02$	$0.55 \pm 0.02 \pm 0.02 \pm 0.02$	$0.63 \pm 0.02 \pm 0.02 \pm 0.02$
[4, 6], [1.8, 2.3]	$0.49 \pm 0.02 \pm 0.02 \pm 0.02$	$0.48 \pm 0.02 \pm 0.02 \pm 0.02$	$0.48 \pm 0.01 \pm 0.02 \pm 0.01$	$0.53 \pm 0.03 \pm 0.02 \pm 0.02$	$0.50 \pm 0.02 \pm 0.02 \pm 0.02$	$0.59 \pm 0.02 \pm 0.02 \pm 0.02$
[4, 6], [2.3, 2.8]	$0.44 \pm 0.01 \pm 0.01 \pm 0.02$	$0.48 \pm 0.02 \pm 0.02 \pm 0.02$	$0.52 \pm 0.02 \pm 0.02 \pm 0.01$	$0.51 \pm 0.02 \pm 0.02 \pm 0.01$	$0.50 \pm 0.02 \pm 0.02 \pm 0.01$	$0.62 \pm 0.02 \pm 0.02 \pm 0.02$
[4, 6], [2.8, 3.3]	$0.46 \pm 0.02 \pm 0.02 \pm 0.02$	$0.47 \pm 0.03 \pm 0.02 \pm 0.01$	$0.49 \pm 0.02 \pm 0.02 \pm 0.01$	$0.56 \pm 0.02 \pm 0.02 \pm 0.01$	$0.51 \pm 0.02 \pm 0.03 \pm 0.01$	$0.59 \pm 0.03 \pm 0.02 \pm 0.02$
[6, 8], [1.8, 2.3]	$0.49 \pm 0.03 \pm 0.03 \pm 0.02$	$0.49 \pm 0.02 \pm 0.03 \pm 0.02$	$0.51 \pm 0.02 \pm 0.03 \pm 0.01$	$0.50 \pm 0.02 \pm 0.03 \pm 0.02$	$0.52 \pm 0.03 \pm 0.02 \pm 0.02$	$0.59 \pm 0.05 \pm 0.02 \pm 0.02$
[6, 8], [2.3, 2.8]	$0.44 \pm 0.03 \pm 0.02 \pm 0.02$	$0.46 \pm 0.03 \pm 0.03 \pm 0.02$	$0.50 \pm 0.02 \pm 0.03 \pm 0.01$	$0.51 \pm 0.02 \pm 0.03 \pm 0.01$	$0.55 \pm 0.04 \pm 0.03 \pm 0.01$	$0.52 \pm 0.07 \pm 0.04 \pm 0.01$
[6, 8], [2.8, 3.3]	$0.48 \pm 0.03 \pm 0.03 \pm 0.02$	$0.48 \pm 0.03 \pm 0.04 \pm 0.01$	$0.47 \pm 0.03 \pm 0.03 \pm 0.01$	$0.51 \pm 0.04 \pm 0.03 \pm 0.01$	$0.53 \pm 0.04 \pm 0.03 \pm 0.01$	$0.61 \pm 0.05 \pm 0.06 \pm 0.02$
[8, 12], [1.8, 2.3]	$0.45 \pm 0.04 \pm 0.04 \pm 0.02$	$0.60 \pm 0.04 \pm 0.04 \pm 0.02$	$0.50 \pm 0.03 \pm 0.03 \pm 0.01$	$0.49 \pm 0.03 \pm 0.03 \pm 0.01$	$0.58 \pm 0.04 \pm 0.03 \pm 0.02$	$0.56 \pm 0.04 \pm 0.03 \pm 0.02$
[8, 12], [2.3, 2.8]	$0.39 \pm 0.03 \pm 0.03 \pm 0.01$	$0.52 \pm 0.04 \pm 0.04 \pm 0.01$	$0.50 \pm 0.06 \pm 0.04 \pm 0.01$	$0.48 \pm 0.04 \pm 0.04 \pm 0.01$	$0.50 \pm 0.04 \pm 0.03 \pm 0.01$	$0.61 \pm 0.04 \pm 0.03 \pm 0.02$
[8, 12], [2.8, 3.3]	$0.39 \pm 0.04 \pm 0.04 \pm 0.01$	$0.43 \pm 0.05 \pm 0.04 \pm 0.01$	$0.42 \pm 0.04 \pm 0.04 \pm 0.01$	$0.54 \pm 0.07 \pm 0.05 \pm 0.02$	$0.57 \pm 0.07 \pm 0.05 \pm 0.02$	$0.59 \pm 0.08 \pm 0.04 \pm 0.02$

$\sigma_{D_s^+}/\sigma_{D^+}$ (Backward)

p_T [GeV/c], y^* \ $N_{\text{tracks}}^{\text{PV}}$	[10, 60]	[60, 80]	[80, 100]	[100, 120]	[120, 140]	[140, 180]	[180, 250]
[2, 4], [−3.3, −2.8]	$0.53 \pm 0.01 \pm 0.03 \pm 0.02$	$0.51 \pm 0.02 \pm 0.04 \pm 0.03$	$0.51 \pm 0.01 \pm 0.02 \pm 0.02$	$0.55 \pm 0.02 \pm 0.02 \pm 0.02$	$0.56 \pm 0.02 \pm 0.02 \pm 0.02$	$0.61 \pm 0.02 \pm 0.02 \pm 0.02$	$0.72 \pm 0.02 \pm 0.04 \pm 0.04$
[2, 4], [−3.8, −3.3]	$0.47 \pm 0.01 \pm 0.02 \pm 0.01$	$0.51 \pm 0.01 \pm 0.03 \pm 0.02$	$0.54 \pm 0.01 \pm 0.03 \pm 0.02$	$0.52 \pm 0.02 \pm 0.02 \pm 0.02$	$0.57 \pm 0.01 \pm 0.03 \pm 0.02$	$0.61 \pm 0.02 \pm 0.02 \pm 0.02$	$0.90 \pm 0.06 \pm 0.03 \pm 0.04$
[2, 4], [−4.3, −3.8]	$0.52 \pm 0.01 \pm 0.03 \pm 0.02$	$0.48 \pm 0.02 \pm 0.03 \pm 0.02$	$0.51 \pm 0.01 \pm 0.03 \pm 0.02$	$0.56 \pm 0.02 \pm 0.03 \pm 0.02$	$0.61 \pm 0.02 \pm 0.03 \pm 0.02$	$0.68 \pm 0.02 \pm 0.04 \pm 0.03$	$0.76 \pm 0.08 \pm 0.03 \pm 0.03$
[4, 6], [−3.3, −2.8]	$0.50 \pm 0.01 \pm 0.03 \pm 0.02$	$0.48 \pm 0.02 \pm 0.03 \pm 0.02$	$0.54 \pm 0.01 \pm 0.03 \pm 0.02$	$0.57 \pm 0.03 \pm 0.02 \pm 0.02$	$0.61 \pm 0.02 \pm 0.02 \pm 0.02$	$0.68 \pm 0.02 \pm 0.02 \pm 0.02$	$0.74 \pm 0.03 \pm 0.02 \pm 0.03$
[4, 6], [−3.8, −3.3]	$0.47 \pm 0.01 \pm 0.03 \pm 0.02$	$0.57 \pm 0.02 \pm 0.04 \pm 0.02$	$0.53 \pm 0.01 \pm 0.03 \pm 0.01$	$0.57 \pm 0.02 \pm 0.03 \pm 0.02$	$0.60 \pm 0.03 \pm 0.03 \pm 0.02$	$0.62 \pm 0.02 \pm 0.02 \pm 0.02$	$0.76 \pm 0.04 \pm 0.02 \pm 0.03$
[4, 6], [−4.3, −3.8]	$0.43 \pm 0.02 \pm 0.03 \pm 0.02$	$0.46 \pm 0.02 \pm 0.03 \pm 0.02$	$0.55 \pm 0.02 \pm 0.04 \pm 0.02$	$0.58 \pm 0.02 \pm 0.04 \pm 0.02$	$0.58 \pm 0.02 \pm 0.03 \pm 0.02$	$0.64 \pm 0.03 \pm 0.03 \pm 0.02$	$0.82 \pm 0.05 \pm 0.03 \pm 0.03$
[6, 8], [−3.3, −2.8]	$0.54 \pm 0.03 \pm 0.05 \pm 0.02$	$0.53 \pm 0.03 \pm 0.05 \pm 0.02$	$0.46 \pm 0.02 \pm 0.04 \pm 0.01$	$0.53 \pm 0.03 \pm 0.03 \pm 0.02$	$0.51 \pm 0.02 \pm 0.03 \pm 0.02$	$0.68 \pm 0.03 \pm 0.03 \pm 0.02$	$0.81 \pm 0.05 \pm 0.06 \pm 0.03$
[6, 8], [−3.8, −3.3]	$0.50 \pm 0.03 \pm 0.05 \pm 0.02$	$0.44 \pm 0.02 \pm 0.04 \pm 0.01$	$0.47 \pm 0.02 \pm 0.04 \pm 0.01$	$0.62 \pm 0.03 \pm 0.05 \pm 0.02$	$0.56 \pm 0.03 \pm 0.03 \pm 0.02$	$0.64 \pm 0.03 \pm 0.03 \pm 0.02$	$0.60 \pm 0.06 \pm 0.11 \pm 0.02$
[6, 8], [−4.3, −3.8]	$0.47 \pm 0.03 \pm 0.06 \pm 0.02$	$0.50 \pm 0.04 \pm 0.07 \pm 0.02$	$0.46 \pm 0.03 \pm 0.05 \pm 0.01$	$0.50 \pm 0.04 \pm 0.05 \pm 0.01$	$0.64 \pm 0.05 \pm 0.06 \pm 0.02$	$0.59 \pm 0.04 \pm 0.04 \pm 0.02$	$0.71 \pm 0.09 \pm 0.05 \pm 0.02$
[8, 12], [−3.3, −2.8]	$0.61 \pm 0.05 \pm 0.08 \pm 0.02$	$0.54 \pm 0.03 \pm 0.07 \pm 0.02$	$0.45 \pm 0.03 \pm 0.04 \pm 0.02$	$0.58 \pm 0.03 \pm 0.05 \pm 0.02$	$0.55 \pm 0.04 \pm 0.05 \pm 0.02$	$0.51 \pm 0.03 \pm 0.03 \pm 0.02$	$0.74 \pm 0.06 \pm 0.05 \pm 0.02$
[8, 12], [−3.8, −3.3]	$0.51 \pm 0.04 \pm 0.08 \pm 0.02$	$0.52 \pm 0.03 \pm 0.07 \pm 0.02$	$0.59 \pm 0.04 \pm 0.07 \pm 0.02$	$0.61 \pm 0.09 \pm 0.06 \pm 0.02$	$0.46 \pm 0.05 \pm 0.04 \pm 0.01$	$0.59 \pm 0.04 \pm 0.04 \pm 0.02$	$0.66 \pm 0.08 \pm 0.07 \pm 0.02$
[8, 12], [−4.3, −3.8]	$0.48 \pm 0.06 \pm 0.11 \pm 0.02$	$0.43 \pm 0.06 \pm 0.09 \pm 0.02$	$0.55 \pm 0.07 \pm 0.10 \pm 0.02$	$0.62 \pm 0.08 \pm 0.11 \pm 0.02$	$0.47 \pm 0.06 \pm 0.08 \pm 0.02$	$0.58 \pm 0.08 \pm 0.07 \pm 0.02$	$0.66 \pm 0.15 \pm 0.07 \pm 0.02$

References

[1] B. R. Webber, *A QCD model for jet fragmentation including soft gluon interference*, Nucl. Phys. **B238** (1984) 492.

[2] B. Andersson, G. Gustafson, G. Ingelman, and T. Sjostrand, *Parton fragmentation and string dynamics*, Phys. Rept. **97** (1983) 31.

[3] M. Hirai, S. Kumano, and T.-H. Nagai, *Determination of nuclear parton distribution functions and their uncertainties in next-to-leading order*, Phys. Rev. **C76** (2007) 065207, `arXiv:0709.3038`.

[4] K. J. Eskola, P. Paakkinen, H. Paukkunen, and C. A. Salgado, *EPPS21: a global QCD analysis of nuclear PDFs*, Eur. Phys. J. **C82** (2022) 413, `arXiv:2112.12462`.

[5] F. Gelis, *Color Glass Condensate and Glasma*, Int. J. Mod. Phys. **A28** (2013) 1330001, `arXiv:1211.3327`.

[6] H. Fujii and K. Watanabe, *Heavy quark pair production in high energy pA collisions: Open heavy flavors*, Nucl. Phys. **A920** (2013) 78, `arXiv:1308.1258`.

[7] LHCb collaboration, I. Bezshyiko *et al.*, *Measurement of the Prompt D0 Nuclear Modification Factor in p-Pb Collisions at sNN=8.16 TeV*, Phys. Rev. Lett. **131** (2023) 102301, `arXiv:2205.03936`.

[8] E. Braaten, K.-m. Cheung, S. Fleming, and T. C. Yuan, *Perturbative QCD fragmentation functions as a model for heavy quark fragmentation*, Phys. Rev. **D51** (1995) 4819, `arXiv:hep-ph/9409316`.

[9] ALICE collaboration, S. Acharya *et al.*, *Charm-quark fragmentation fractions and production cross section at midrapidity in pp collisions at the LHC*, Phys. Rev. **D105** (2022) L011103, `arXiv:2105.06335`.

[10] ALICE collaboration, S. Acharya *et al.*, *Charm production and fragmentation fractions at midrapidity in pp collisions at $\sqrt{s} = 13$ TeV*, `arXiv:2308.04877`.

[11] Y. Oh, C. M. Ko, S. H. Lee, and S. Yasui, *Heavy baryon/meson ratios in relativistic heavy ion collisions*, Phys. Rev. **C79** (2009) 044905, `arXiv:0901.1382`.

[12] M. He and R. Rapp, *Hadronization and charm-hadron ratios in heavy-ion collisions*, Phys. Rev. Lett. **124** (2020) 042301, `arXiv:1905.09216`.

[13] V. Minissale, S. Plumari, and V. Greco, *Charm hadrons in pp collisions at LHC energy within a coalescence plus fragmentation approach*, Phys. Lett. **B821** (2021) 136622, `arXiv:2012.12001`.

[14] CMS collaboration, A. M. Sirunyan *et al.*, *Elliptic flow of charm and strange hadrons in high-multiplicity pPb collisions at $\sqrt{s_{\mathrm{NN}}} = 8.16$ TeV*, Phys. Rev. Lett. **121** (2018) 082301, `arXiv:1804.09767`.

[15] STAR collaboration, J. Adams *et al.*, *Experimental and theoretical challenges in the search for the quark gluon plasma: The STAR Collaboration's critical assessment of the evidence from RHIC collisions*, Nucl. Phys. **A757** (2005) 102, `arXiv:nucl-ex/0501009`.

[16] PHENIX collaboration, K. Adcox *et al.*, *Formation of dense partonic matter in relativistic nucleus-nucleus collisions at RHIC: Experimental evaluation by the PHENIX collaboration*, Nucl. Phys. **A757** (2005) 184, `arXiv:nucl-ex/0410003`.

[17] J. Rafelski and B. Müller, *Strangeness production in the quark-gluon plasma*, Phys. Rev. Lett. **48** (1982) 1066.

[18] STAR collaboration, G. Agakishiev *et al.*, *Strangeness enhancement in Cu+Cu and Au+Au collisions at $\sqrt{s_{NN}} = 200$ GeV*, Phys. Rev. Lett. **108** (2012) 072301, `arXiv:1107.2955`.

[19] ALICE collaboration, B. B. Abelev *et al.*, *Multi-strange baryon production at midrapidity in Pb-Pb collisions at $\sqrt{s_{NN}} = 2.76$ TeV*, Phys. Lett. **B728** (2014) 216, Erratum ibid. **734** (2014) 409, `arXiv:1307.5543`.

[20] STAR collaboration, J. Adam *et al.*, *Observation of $D_s^{\pm}/D^0$ enhancement in Au+Au collisions at $\sqrt{s_{NN}} = 200$ GeV*, Phys. Rev. Lett. **127** (2021) 092301, `arXiv:2101.11793`.

[21] ALICE collaboration, S. Acharya *et al.*, *Measurement of prompt D_s^+-meson production and azimuthal anisotropy in Pb–Pb collisions at $\sqrt{s_{NN}}=5.02TeV$*, Phys. Lett. **B827** (2022) 136986, `arXiv:2110.10006`.

[22] ALICE collaboration, J. Adam *et al.*, *Enhanced production of multi-strange hadrons in high-multiplicity proton-proton collisions*, Nature Phys. **13** (2017) 535, `arXiv:1606.07424`.

[23] ALICE collaboration, B. B. Abelev *et al.*, *Multiplicity dependence of pion, kaon, proton and lambda production in p-Pb collisions at $\sqrt{s_{NN}} = 5.02$ TeV*, Phys. Lett. **B728** (2014) 25, `arXiv:1307.6796`.

[24] ALICE collaboration, J. Adam *et al.*, *Multi-strange baryon production in p-Pb collisions at $\sqrt{s_{NN}} = 5.02$ TeV*, Phys. Lett. **B758** (2016) 389, `arXiv:1512.07227`.

[25] Y. Kanakubo, Y. Tachibana, and T. Hirano, *Unified description of hadron yield ratios from dynamical core-corona initialization*, Phys. Rev. **C101** (2020) 024912, `arXiv:1910.10556`.

[26] C. Bierlich, S. Chakraborty, G. Gustafson, and L. Lönnblad, *Strangeness enhancement across collision systems without a plasma*, Phys. Lett. **B835** (2022) 137571, `arXiv:2205.11170`.

[27] LHCb collaboration, A. A. Alves Jr. *et al.*, *The LHCb detector at the LHC*, JINST **3** (2008) S08005.

[28] LHCb collaboration, R. Aaij *et al.*, *LHCb detector performance*, Int. J. Mod. Phys. **A30** (2015) 1530022, `arXiv:1412.6352`.

[29] T. Sjöstrand, S. Mrenna, and P. Skands, *A brief introduction to PYTHIA 8.1*, Comput. Phys. Commun. **178** (2008) 852, `arXiv:0710.3820`; T. Sjöstrand, S. Mrenna, and P. Skands, *PYTHIA 6.4 physics and manual*, JHEP **05** (2006) 026, `arXiv:hep-ph/0603175`.

[30] T. Pierog *et al.*, *EPOS LHC: Test of collective hadronization with data measured at the CERN Large Hadron Collider*, Phys. Rev. **C92** (2015) 034906, `arXiv:1306.0121`.

[31] LHCb collaboration, I. Belyaev *et al.*, *Handling of the generation of primary events in Gauss, the LHCb simulation framework*, J. Phys. Conf. Ser. **331** (2011) 032047.

[32] D. J. Lange, *The EvtGen particle decay simulation package*, Nucl. Instrum. Meth. **A462** (2001) 152.

[33] P. Golonka and Z. Was, *PHOTOS Monte Carlo: A precision tool for QED corrections in Z and W decays*, Eur. Phys. J. **C45** (2006) 97, `arXiv:hep-ph/0506026`.

[34] GEANT4 collaboration, S. Agostinelli *et al.*, *GEANT4–a simulation toolkit*, Nucl. Instrum. Meth. **A506** (2003) 250.

[35] LHCb collaboration, M. Clemencic *et al.*, *The LHCb simulation application, Gauss: Design, evolution and experience*, J. Phys. Conf. Ser. **331** (2011) 032023.

[36] M. Pivk and F. R. Le Diberder, *sPlot: A statistical tool to unfold data distributions*, Nucl. Instrum. Meth. **A555** (2005) 356, `arXiv:physics/0402083`.

[37] CLEO collaboration, J. P. Alexander *et al.*, *Absolute measurement of hadronic branching fractions of the D_s^+ meson*, Phys. Rev. Lett. **100** (2008) 161804, `arXiv:0801.0680`.

[38] Particle Data Group, R. L. Workman *et al.*, *Review of Particle Physics*, PTEP **2022** (2022) 083C01.

[39] T. Skwarnicki, *A study of the radiative cascade transitions between the Upsilon-prime and Upsilon resonances*, PhD thesis, Institute of Nuclear Physics, Krakow, 1986, DESY-F31-86-02.

[40] A. D. Bukin, *Fitting function for asymmetric peaks*, `arXiv:0711.4449`.

[41] R. Aaij *et al.*, *See Supplemental Material at [URL to be added] for further details*, .

[42] LHCb collaboration, R. Aaij *et al.*, *Measurement of the track reconstruction efficiency at LHCb*, JINST **10** (2015) P02007, `arXiv:1408.1251`.

[43] L. Anderlini *et al.*, *The PIDCalib package*, LHCb-PUB-2016-021, 2016.

[44] R. Aaij *et al.*, *Selection and processing of calibration samples to measure the particle identification performance of the LHCb experiment in Run 2*, Eur. Phys. J. Tech. Instr. **6** (2019) 1, `arXiv:1803.00824`.

[45] LHCb collaboration, I. Bezshyiko *et al.*, *Measurement of prompt D^+ and D_s^+ production in pPb collisions at $\sqrt{s_{NN}} = 5.02$ TeV*, JHEP **01** (2024) 070, `arXiv:2309.14206`.
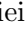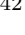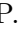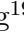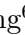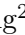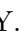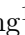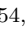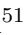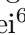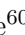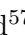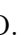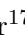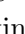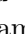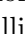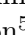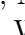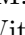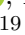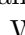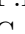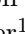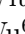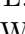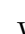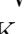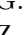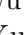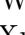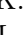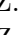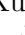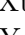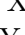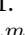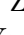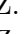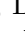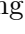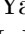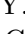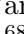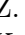
[46] S. Tolk, J. Albrecht, F. Dettori, and A. Pellegrino, *Data driven trigger efficiency determination at LHCb*, LHCb-PUB-2014-039, 2014.

[47] LHCb collaboration, R. Aaij *et al.*, *Measurements of prompt charm production cross-sections in pp collisions at $\sqrt{s} = 5\,TeV$*, JHEP **06** (2017) 147, arXiv:1610.02230.

[48] LHCb collaboration, R. Aaij *et al.*, *Measurements of prompt charm production cross-sections in pp collisions at $\sqrt{s} = 13\,TeV$*, JHEP **03** (2016) 159, Erratum ibid. **09** (2016) 013, Erratum ibid. **05** (2017) 074, arXiv:1510.01707.

[49] H.-S. Shao, *HELAC-Onia: An automatic matrix element generator for heavy quarkonium physics*, Comput. Phys. Commun. **184** (2013) 2562, arXiv:1212.5293.

[50] H.-S. Shao, *HELAC-Onia 2.0: an upgraded matrix-element and event generator for heavy quarkonium physics*, Comput. Phys. Commun. **198** (2016) 238, arXiv:1507.03435.

[51] J.-P. Lansberg and H.-S. Shao, *Towards an automated tool to evaluate the impact of the nuclear modification of the gluon density on quarkonium, D and B meson production in proton–nucleus collisions*, Eur. Phys. J. **C77** (2017) 1, arXiv:1610.05382.

[52] K. J. Eskola, P. Paakkinen, H. Paukkunen, and C. A. Salgado, *EPPS16: Nuclear parton distributions with LHC data*, Eur. Phys. J. **C77** (2017) 163, arXiv:1612.05741.

[53] K. Kovarik *et al.*, *nCTEQ15 - Global analysis of nuclear parton distributions with uncertainties in the CTEQ framework*, Phys. Rev. **D93** (2016) 085037, arXiv:1509.00792.

[54] LHCb collaboration, R. Aaij *et al.*, *Study of prompt D^0 meson production in pPb collisions at $\sqrt{s_{NN}} = 5\,TeV$*, JHEP **10** (2017) 090, arXiv:1707.02750.

[55] ALICE collaboration, B. B. Abelev *et al.*, *Measurement of prompt D-meson production in $p - Pb$ collisions at $\sqrt{s_{NN}} = 5.02\,TeV$*, Phys. Rev. Lett. **113** (2014) 232301, arXiv:1405.3452.

[56] ALICE collaboration, J. Adam *et al.*, *Measurement of D-meson production versus multiplicity in p-Pb collisions at $\sqrt{s_{NN}} = 5.02\,TeV$*, JHEP **08** (2016) 078, arXiv:1602.07240.

[57] ALICE collaboration, J. Adam *et al.*, *D-meson production in p-Pb collisions at $\sqrt{s_{NN}} = 5.02\,TeV$ and in pp collisions at $\sqrt{s} = 7\,TeV$*, Phys. Rev. **C94** (2016) 054908, arXiv:1605.07569.

[58] A. Kusina, J.-P. Lansberg, I. Schienbein, and H.-S. Shao, *Gluon shadowing in heavy-flavor production at the LHC*, Phys. Rev. Lett. **121** (2018) 052004, arXiv:1712.07024.

[59] B. Ducloué, T. Lappi, and H. Mäntysaari, *Forward J/ψ production in proton-nucleus collisions at high energy*, Phys. Rev. **D91** (2015) 114005, arXiv:1503.02789.

[60] B. Ducloué, T. Lappi, and H. Mäntysaari, *Forward J/ψ and D meson nuclear suppression at the LHC*, Nucl. Part. Phys. Proc. **289-290** (2017) 309, arXiv:1612.04585.

[61] Y.-Q. Ma, P. Tribedy, R. Venugopalan, and K. Watanabe, *Event engineering studies for heavy flavor production and hadronization in high multiplicity hadron-hadron and hadron-nucleus collisions*, Phys. Rev. **D98** (2018) 074025, `arXiv:1803.11093`.

[62] M. Lisovyi, A. Verbytskyi, and O. Zenaiev, *Combined analysis of charm-quark fragmentation-fraction measurements*, Eur. Phys. J. C **76** (2016) 397, `arXiv:1509.01061`.

[63] LHCb collaboration, R. Aaij *et al.*, *Measurements of prompt charm production cross-sections in pp collisions at $\sqrt{s} = 5$ TeV*, JHEP **06** (2017) 147, `arXiv:1610.02230`.

[64] ALICE collaboration, S. Acharya *et al.*, *Measurement of prompt D^0, D^+, D^{*+}, and D_S^+ production in p–Pb collisions at $\sqrt{s_{NN}} = 5.02$ TeV*, JHEP **12** (2019) 092, `arXiv:1906.03425`.

[65] ALICE collaboration, S. Acharya *et al.*, *Measurement of D^0, D^+, D^{*+} and D_s^+ production in Pb-Pb collisions at $\sqrt{s_{NN}} = 5.02$ TeV*, JHEP **10** (2018) 174, `arXiv:1804.09083`.

[66] P. Skands, S. Carrazza, and J. Rojo, *Tuning PYTHIA 8.1: the Monash 2013 Tune*, Eur. Phys. J. C **74** (2014) 3024, `arXiv:1404.5630`.

[67] J. R. Christiansen and P. Z. Skands, *String Formation Beyond Leading Colour*, JHEP **08** (2015) 003, `arXiv:1505.01681`.

[68] J. Zhao, J. Aichelin, P. B. Gossiaux, and K. Werner, *Heavy flavor as a probe of hot QCD matter produced in proton-proton collisions*, `arXiv:2310.08684`.

[69] J. Zhao, J. Aichelin, P. B. Gossiaux, and K. Werner, *Heavy flavour hadron production in relativistic heavy ion collisions at RHIC and LHC in EPOS4HQ*, `arXiv:2401.17096`.

LHCb collaboration

R. Aaij[35] ⓘ, A.S.W. Abdelmotteleb[54] ⓘ, C. Abellan Beteta[48], F. Abudinén[54] ⓘ,
T. Ackernley[58] ⓘ, B. Adeva[44] ⓘ, M. Adinolfi[52] ⓘ, P. Adlarson[78] ⓘ, H. Afsharnia[11],
C. Agapopoulou[46] ⓘ, C.A. Aidala[79] ⓘ, Z. Ajaltouni[11], S. Akar[63] ⓘ, K. Akiba[35] ⓘ,
P. Albicocco[25] ⓘ, J. Albrecht[17] ⓘ, F. Alessio[46] ⓘ, M. Alexander[57] ⓘ, A. Alfonso Albero[43] ⓘ,
Z. Aliouche[60] ⓘ, P. Alvarez Cartelle[53] ⓘ, R. Amalric[15] ⓘ, S. Amato[3] ⓘ, J.L. Amey[52] ⓘ,
Y. Amhis[13,46] ⓘ, L. An[6] ⓘ, L. Anderlini[24] ⓘ, M. Andersson[48] ⓘ, A. Andreianov[41] ⓘ,
P. Andreola[48] ⓘ, M. Andreotti[23] ⓘ, D. Andreou[66] ⓘ, D. Ao[7] ⓘ, F. Archilli[34,u] ⓘ,
S. Arguedas Cuendis[9] ⓘ, A. Artamonov[41] ⓘ, M. Artuso[66] ⓘ, E. Aslanides[12] ⓘ, M. Atzeni[62] ⓘ,
B. Audurier[14] ⓘ, D. Bacher[61] ⓘ, I. Bachiller Perea[10] ⓘ, S. Bachmann[19] ⓘ, M. Bachmayer[47] ⓘ,
J.J. Back[54] ⓘ, A. Bailly-reyre[15], P. Baladron Rodriguez[44] ⓘ, V. Balagura[14] ⓘ,
W. Baldini[23,46] ⓘ, J. Baptista de Souza Leite[2] ⓘ, M. Barbetti[24,l] ⓘ, I. R. Barbosa[67] ⓘ,
R.J. Barlow[60] ⓘ, S. Barsuk[13] ⓘ, W. Barter[56] ⓘ, M. Bartolini[53] ⓘ, F. Baryshnikov[41] ⓘ,
J.M. Basels[16] ⓘ, G. Bassi[32,r] ⓘ, B. Batsukh[5] ⓘ, A. Battig[17] ⓘ, A. Bay[47] ⓘ, A. Beck[54] ⓘ,
M. Becker[17] ⓘ, F. Bedeschi[32] ⓘ, I.B. Bediaga[2] ⓘ, A. Beiter[66], S. Belin[44] ⓘ, V. Bellee[48] ⓘ,
K. Belous[41] ⓘ, I. Belov[26] ⓘ, I. Belyaev[41] ⓘ, G. Benane[12] ⓘ, G. Bencivenni[25] ⓘ,
E. Ben-Haim[15] ⓘ, A. Berezhnoy[41] ⓘ, R. Bernet[48] ⓘ, S. Bernet Andres[42] ⓘ, D. Berninghoff[19],
H.C. Bernstein[66], C. Bertella[60] ⓘ, A. Bertolin[30] ⓘ, C. Betancourt[48] ⓘ, F. Betti[56] ⓘ, J.
Bex[53] ⓘ, Ia. Bezshyiko[48] ⓘ, J. Bhom[38] ⓘ, L. Bian[71] ⓘ, M.S. Bieker[17] ⓘ, N.V. Biesuz[23] ⓘ,
P. Billoir[15] ⓘ, A. Biolchini[35] ⓘ, M. Birch[59] ⓘ, F.C.R. Bishop[53] ⓘ, A. Bitadze[60] ⓘ, A. Bizzeti ⓘ,
M.P. Blago[53] ⓘ, T. Blake[54] ⓘ, F. Blanc[47] ⓘ, J.E. Blank[17] ⓘ, S. Blusk[66] ⓘ, D. Bobulska[57] ⓘ,
V. Bocharnikov[41] ⓘ, J.A. Boelhauve[17] ⓘ, O. Boente Garcia[14] ⓘ, T. Boettcher[63] ⓘ, A.
Bohare[56] ⓘ, A. Boldyrev[41] ⓘ, C.S. Bolognani[76] ⓘ, R. Bolzonella[23,k] ⓘ, N. Bondar[41] ⓘ,
F. Borgato[30,46] ⓘ, S. Borghi[60] ⓘ, M. Borsato[28,o] ⓘ, J.T. Borsuk[38] ⓘ, S.A. Bouchiba[47] ⓘ,
T.J.V. Bowcock[58] ⓘ, A. Boyer[46] ⓘ, C. Bozzi[23] ⓘ, M.J. Bradley[59], S. Braun[64] ⓘ,
A. Brea Rodriguez[44] ⓘ, N. Breer[17] ⓘ, J. Brodzicka[38] ⓘ, A. Brossa Gonzalo[44] ⓘ, J. Brown[58] ⓘ,
D. Brundu[29] ⓘ, A. Buonaura[48] ⓘ, L. Buonincontri[30] ⓘ, A.T. Burke[60] ⓘ, C. Burr[46] ⓘ,
A. Bursche[69], A. Butkevich[41] ⓘ, J.S. Butter[53] ⓘ, J. Buytaert[46] ⓘ, W. Byczynski[46] ⓘ,
S. Cadeddu[29] ⓘ, H. Cai[71], R. Calabrese[23,k] ⓘ, L. Calefice[17] ⓘ, S. Cali[25] ⓘ, M. Calvi[28,o] ⓘ,
M. Calvo Gomez[42] ⓘ, J. Cambon Bouzas[44] ⓘ, P. Campana[25] ⓘ, D.H. Campora Perez[76] ⓘ,
A.F. Campoverde Quezada[7] ⓘ, S. Capelli[28,o] ⓘ, L. Capriotti[23] ⓘ, A. Carbone[22,i] ⓘ,
L. Carcedo Salgado[44] ⓘ, R. Cardinale[26,m] ⓘ, A. Cardini[29] ⓘ, P. Carniti[28,o] ⓘ, L. Carus[19],
A. Casais Vidal[44] ⓘ, R. Caspary[19] ⓘ, G. Casse[58] ⓘ, J. Castro Godinez[9] ⓘ, M. Cattaneo[46] ⓘ,
G. Cavallero[23] ⓘ, V. Cavallini[23,k] ⓘ, S. Celani[47] ⓘ, J. Cerasoli[12] ⓘ, D. Cervenkov[61] ⓘ, S.
Cesare[27,n] ⓘ, A.J. Chadwick[58] ⓘ, I. Chahrour[79] ⓘ, M.G. Chapman[52], M. Charles[15] ⓘ,
Ph. Charpentier[46] ⓘ, C.A. Chavez Barajas[58] ⓘ, M. Chefdeville[10] ⓘ, C. Chen[12] ⓘ, S. Chen[5] ⓘ,
A. Chernov[38] ⓘ, S. Chernyshenko[50] ⓘ, V. Chobanova[44,y] ⓘ, S. Cholak[47] ⓘ, M. Chrzaszcz[38] ⓘ,
A. Chubykin[41] ⓘ, V. Chulikov[41] ⓘ, P. Ciambrone[25] ⓘ, M.F. Cicala[54] ⓘ, X. Cid Vidal[44] ⓘ,
G. Ciezarek[46] ⓘ, P. Cifra[46] ⓘ, P.E.L. Clarke[56] ⓘ, M. Clemencic[46] ⓘ, H.V. Cliff[53] ⓘ,
J. Closier[46] ⓘ, J.L. Cobbledick[60] ⓘ, C. Cocha Toapaxi[19] ⓘ, V. Coco[46] ⓘ, J. Cogan[12] ⓘ,
E. Cogneras[11] ⓘ, L. Cojocariu[40] ⓘ, P. Collins[46] ⓘ, T. Colombo[46] ⓘ, A. Comerma-Montells[43] ⓘ,
L. Congedo[21] ⓘ, A. Contu[29] ⓘ, N. Cooke[57] ⓘ, I. Corredoira [44] ⓘ, A. Correia[15] ⓘ, G. Corti[46] ⓘ,
J.J. Cottee Meldrum[52], B. Couturier[46] ⓘ, D.C. Craik[48] ⓘ, M. Cruz Torres[2,g] ⓘ, R. Currie[56] ⓘ,
C.L. Da Silva[65] ⓘ, S. Dadabaev[41] ⓘ, L. Dai[68] ⓘ, X. Dai[6] ⓘ, E. Dall'Occo[17] ⓘ, J. Dalseno[44] ⓘ,
C. D'Ambrosio[46] ⓘ, J. Daniel[11] ⓘ, A. Danilina[41] ⓘ, P. d'Argent[21] ⓘ, A. Davidson[54] ⓘ,
J.E. Davies[60] ⓘ, A. Davis[60] ⓘ, O. De Aguiar Francisco[60] ⓘ, C. De Angelis[29,j], J. de Boer[35] ⓘ,
K. De Bruyn[75] ⓘ, S. De Capua[60] ⓘ, M. De Cian[19] ⓘ, U. De Freitas Carneiro Da Graca[2,b] ⓘ,
E. De Lucia[25] ⓘ, J.M. De Miranda[2] ⓘ, L. De Paula[3] ⓘ, M. De Serio[21,h] ⓘ, D. De Simone[48] ⓘ,
P. De Simone[25] ⓘ, F. De Vellis[17] ⓘ, J.A. de Vries[76] ⓘ, F. Debernardis[21,h] ⓘ, D. Decamp[10] ⓘ,

V. Dedu[12] , L. Del Buono[15] , B. Delaney[62] , H.-P. Dembinski[17] , J. Deng[8] ,
V. Denysenko[48] , O. Deschamps[11] , F. Dettori[29,j] , B. Dey[74] , P. Di Nezza[25] ,
I. Diachkov[41] , S. Didenko[41] , S. Ding[66] , V. Dobishuk[50] , A. D. Docheva[57] ,
A. Dolmatov[41] , C. Dong[4] , A.M. Donohoe[20] , F. Dordei[29] , A.C. dos Reis[2] ,
L. Douglas[57], A.G. Downes[10] , W. Duan[69] , P. Duda[77] , M.W. Dudek[38] , L. Dufour[46] ,
V. Duk[31] , P. Durante[46] , M. M. Duras[77] , J.M. Durham[65] , D. Dutta[60] ,
A. Dziurda[38] , A. Dzyuba[41] , S. Easo[55,46] , E. Eckstein[73], U. Egede[1] , A. Egorychev[41] ,
V. Egorychev[41] , C. Eirea Orro[44], S. Eisenhardt[56] , E. Ejopu[60] , S. Ek-In[47] ,
L. Eklund[78] , M. Elashri[63] , J. Ellbracht[17] , S. Ely[59] , A. Ene[40] , E. Epple[63] ,
S. Escher[16] , J. Eschle[48] , S. Esen[48] , T. Evans[60] , F. Fabiano[29,j,46] , L.N. Falcao[2] ,
Y. Fan[7] , B. Fang[71,13] , L. Fantini[31,q] , M. Faria[47] , K. Farmer[56] , D. Fazzini[28,o] ,
L. Felkowski[77] , M. Feng[5,7] , M. Feo[46] , M. Fernandez Gomez[44] , A.D. Fernez[64] ,
F. Ferrari[22] , F. Ferreira Rodrigues[3] , S. Ferreres Sole[35] , M. Ferrillo[48] ,
M. Ferro-Luzzi[46] , S. Filippov[41] , R.A. Fini[21] , M. Fiorini[23,k] , M. Firlej[37] ,
K.M. Fischer[61] , D.S. Fitzgerald[79] , C. Fitzpatrick[60] , T. Fiutowski[37] , F. Fleuret[14] ,
M. Fontana[22] , F. Fontanelli[26,m] , L. F. Foreman[60] , R. Forty[46] , D. Foulds-Holt[53] ,
M. Franco Sevilla[64] , M. Frank[46] , E. Franzoso[23,k] , G. Frau[19] , C. Frei[46] ,
D.A. Friday[60] , L. Frontini[27,n] , J. Fu[7] , Q. Fuehring[17] , Y. Fujii[1] , T. Fulghesu[15] ,
E. Gabriel[35] , G. Galati[21,h] , M.D. Galati[35] , A. Gallas Torreira[44] , D. Galli[22,i] ,
S. Gambetta[56,46] , M. Gandelman[3] , P. Gandini[27] , H. Gao[7] , R. Gao[61] , Y. Gao[8] ,
Y. Gao[6] , Y. Gao[8], M. Garau[29,j] , L.M. Garcia Martin[47] , P. Garcia Moreno[43] ,
J. García Pardiñas[46] , B. Garcia Plana[44], F.A. Garcia Rosales[14] , L. Garrido[43] ,
C. Gaspar[46] , R.E. Geertsema[35] , L.L. Gerken[17] , E. Gersabeck[60] , M. Gersabeck[60] ,
T. Gershon[54] , Z. Ghorbanimoghaddam[52], L. Giambastiani[30] , F. I. Giasemis[15,e] ,
V. Gibson[53] , H.K. Giemza[39] , A.L. Gilman[61] , M. Giovannetti[25] , A. Gioventù[43] ,
P. Gironella Gironell[43] , C. Giugliano[23,k] , M.A. Giza[38] , K. Gizdov[56] ,
E.L. Gkougkousis[59] , F.C. Glaser[13,19] , V.V. Gligorov[15] , C. Göbel[67] ,
E. Golobardes[42] , D. Golubkov[41] , A. Golutvin[59,41,46] , A. Gomes[2,a,†] ,
S. Gomez Fernandez[43] , F. Goncalves Abrantes[61] , M. Goncerz[38] , G. Gong[4] , J.
A. Gooding[17] , I.V. Gorelov[41] , C. Gotti[28] , J.P. Grabowski[73] ,
L.A. Granado Cardoso[46] , E. Graugés[43] , E. Graverini[47] , L. Grazette[54] , G. Graziani ,
A. T. Grecu[40] , L.M. Greeven[35] , N.A. Grieser[63] , L. Grillo[57] , S. Gromov[41] , C.
Gu[14] , M. Guarise[23] , M. Guittiere[13] , V. Guliaeva[41] , P. A. Günther[19] ,
A.-K. Guseinov[41] , E. Gushchin[41] , Y. Guz[6,41,46] , T. Gys[46] , T. Hadavizadeh[1] ,
C. Hadjivasiliou[64] , G. Haefeli[47] , C. Haen[46] , J. Haimberger[46] , S.C. Haines[53] ,
M. Hajheidari[46], T. Halewood-leagas[58] , M.M. Halvorsen[46] , P.M. Hamilton[64] ,
J. Hammerich[58] , Q. Han[8] , X. Han[19] , S. Hansmann-Menzemer[19] , L. Hao[7] ,
N. Harnew[61] , T. Harrison[58] , M. Hartmann[13] , C. Hasse[46] , J. He[7,d] , K. Heijhoff[35] ,
F. Hemmer[46] , C. Henderson[63] , R.D.L. Henderson[1,54] , A.M. Hennequin[46] ,
K. Hennessy[58] , L. Henry[47] , J. Herd[59] , J. Heuel[16] , A. Hicheur[3] , D. Hill[47] ,
M. Hilton[60] , S.E. Hollitt[17] , J. Horswill[60] , R. Hou[8] , Y. Hou[10] , N. Howarth[58],
J. Hu[19], J. Hu[69] , W. Hu[6] , X. Hu[4] , W. Huang[7] , X. Huang[71], W. Hulsbergen[35] ,
R.J. Hunter[54] , M. Hushchyn[41] , D. Hutchcroft[58] , P. Ibis[17] , M. Idzik[37] , D. Ilin[41] ,
P. Ilten[63] , A. Inglessi[41] , A. Iniukhin[41] , A. Ishteev[41] , K. Ivshin[41] , R. Jacobsson[46] ,
H. Jage[16] , S.J. Jaimes Elles[45,72] , S. Jakobsen[46] , E. Jans[35] , B.K. Jashal[45] ,
A. Jawahery[64] , V. Jevtic[17] , E. Jiang[64] , X. Jiang[5,7] , Y. Jiang[7] , Y. J. Jiang[6] ,
M. John[61] , D. Johnson[51] , C.R. Jones[53] , T.P. Jones[54] , S. Joshi[39] , B. Jost[46] ,
N. Jurik[46] , I. Juszczak[38] , D. Kaminaris[47] , S. Kandybei[49] , Y. Kang[4] ,
M. Karacson[46] , D. Karpenkov[41] , M. Karpov[41] , A. M. Kauniskangas[47] ,
J.W. Kautz[63] , F. Keizer[46] , D.M. Keller[66] , M. Kenzie[53] , T. Ketel[35] , B. Khanji[66] ,

A. Kharisova[41] , S. Kholodenko[32] , G. Khreich[13] , T. Kirn[16] , V.S. Kirsebom[47] ,
O. Kitouni[62] , S. Klaver[36] , N. Kleijne[32,r] , K. Klimaszewski[39] , M.R. Kmiec[39] ,
S. Koliiev[50] , L. Kolk[17] , A. Konoplyannikov[41] , P. Kopciewicz[37,46] , P. Koppenburg[35] ,
M. Korolev[41] , I. Kostiuk[35] , O. Kot[50], S. Kotriakhova , A. Kozachuk[41] ,
P. Kravchenko[41] , L. Kravchuk[41] , M. Kreps[54] , S. Kretzschmar[16] , P. Krokovny[41] ,
W. Krupa[66] , W. Krzemien[39] , J. Kubat[19], S. Kubis[77] , W. Kucewicz[38] ,
M. Kucharczyk[38] , V. Kudryavtsev[41] , E. Kulikova[41] , A. Kupsc[78] , B. K. Kutsenko[12] ,
D. Lacarrere[46] , G. Lafferty[60] , A. Lai[29] , A. Lampis[29,j] , D. Lancierini[48] ,
C. Landesa Gomez[44] , J.J. Lane[1] , R. Lane[52] , C. Langenbruch[19] , J. Langer[17] ,
O. Lantwin[41] , T. Latham[54] , F. Lazzari[32,s] , C. Lazzeroni[51] , R. Le Gac[12] ,
S.H. Lee[79] , R. Lefèvre[11] , A. Leflat[41] , S. Legotin[41] , M. Lehuraux[54] , O. Leroy[12] ,
T. Lesiak[38] , B. Leverington[19] , A. Li[4] , H. Li[69] , K. Li[8] , L. Li[60] , P. Li[46] ,
P.-R. Li[70] , S. Li[8] , T. Li[5] , T. Li[69] , Y. Li[8] , Y. Li[5] , Z. Li[66] , Z. Lian[4] ,
X. Liang[66] , C. Lin[7] , T. Lin[55] , R. Lindner[46] , V. Lisovskyi[47] , R. Litvinov[29,j] ,
G. Liu[69] , H. Liu[7] , K. Liu[70] , Q. Liu[7] , S. Liu[5,7] , Y. Liu[56] , Y. Liu[70],
A. Lobo Salvia[43] , A. Loi[29] , J. Lomba Castro[44] , T. Long[53] , I. Longstaff[57],
J.H. Lopes[3] , A. Lopez Huertas[43] , S. López Soliño[44] , G.H. Lovell[53] , Y. Lu[5,c] ,
C. Lucarelli[24,l] , D. Lucchesi[30,p] , S. Luchuk[41] , M. Lucio Martinez[76] ,
V. Lukashenko[35,50] , Y. Luo[4] , A. Lupato[30] , E. Luppi[23,k] , K. Lynch[20] , X.-R. Lyu[7] ,
G. M. Ma[4] , R. Ma[7] , S. Maccolini[17] , F. Machefert[13] , F. Maciuc[40] , I. Mackay[61] ,
L.R. Madhan Mohan[53] , M. M. Madurai[51] , A. Maevskiy[41] , D. Magdalinski[35] ,
D. Maisuzenko[41] , M.W. Majewski[37], J.J. Malczewski[38] , S. Malde[61] , B. Malecki[38,46] ,
L. Malentacca[46], A. Malinin[41] , T. Maltsev[41] , G. Manca[29,j] , G. Mancinelli[12] ,
C. Mancuso[27,13,n] , R. Manera Escalero[43], D. Manuzzi[22] , D. Marangotto[27,n] ,
J.F. Marchand[10] , U. Marconi[22] , S. Mariani[46] , C. Marin Benito[43,46] , J. Marks[19] ,
A.M. Marshall[52] , P.J. Marshall[58], G. Martelli[31,q] , G. Martellotti[33] , L. Martinazzoli[46] ,
M. Martinelli[28,o] , D. Martinez Santos[44] , F. Martinez Vidal[45] , A. Massafferri[2] ,
M. Materok[16] , R. Matev[46] , A. Mathad[48] , V. Matiunin[41] , C. Matteuzzi[66,28] ,
K.R. Mattioli[14] , A. Mauri[59] , E. Maurice[14] , J. Mauricio[43] , M. Mazurek[46] ,
M. McCann[59] , L. Mcconnell[20] , T.H. McGrath[60] , N.T. McHugh[57] , A. McNab[60] ,
R. McNulty[20] , B. Meadows[63] , G. Meier[17] , D. Melnychuk[39] , M. Merk[35,76] ,
A. Merli[27,n] , L. Meyer Garcia[3] , D. Miao[5,7] , H. Miao[7] , M. Mikhasenko[73,f] ,
D.A. Milanes[72] , A. Minotti[28,o] , E. Minucci[66] , T. Miralles[11] , S.E. Mitchell[56] ,
B. Mitreska[17] , D.S. Mitzel[17] , A. Modak[55] , A. Mödden [17] , R.A. Mohammed[61] ,
R.D. Moise[16] , S. Mokhnenko[41] , T. Mombächer[46] , M. Monk[54,1] , I.A. Monroy[72] ,
S. Monteil[11] , A. Morcillo Gomez[44] , G. Morello[25] , M.J. Morello[32,r] ,
M.P. Morgenthaler[19] , J. Moron[37] , A.B. Morris[46] , A.G. Morris[12] , R. Mountain[66] ,
H. Mu[4] , Z. M. Mu[6] , E. Muhammad[54] , F. Muheim[56] , M. Mulder[75] , K. Müller[48] ,
F. Muñoz-Rojas[9] , R. Murta[59] , P. Naik[58] , T. Nakada[47] , R. Nandakumar[55] ,
T. Nanut[46] , I. Nasteva[3] , M. Needham[56] , N. Neri[27,n] , S. Neubert[73] , N. Neufeld[46] ,
P. Neustroev[41], R. Newcombe[59], J. Nicolini[17,13] , D. Nicotra[76] , E.M. Niel[47] ,
N. Nikitin[41] , P. Nogga[73], N.S. Nolte[62] , C. Normand[10,j,29] , J. Novoa Fernandez[44] ,
G. Nowak[63] , C. Nunez[79] , H. N. Nur[57] , A. Oblakowska-Mucha[37] , V. Obraztsov[41] ,
T. Oeser[16] , S. Okamura[23,k,46] , R. Oldeman[29,j] , F. Oliva[56] , M. Olocco[17] ,
C.J.G. Onderwater[76] , R.H. O'Neil[56] , J.M. Otalora Goicochea[3] , T. Ovsiannikova[41] ,
P. Owen[48] , A. Oyanguren[45] , O. Ozcelik[56] , K.O. Padeken[73] , B. Pagare[54] ,
P.R. Pais[19] , T. Pajero[61] , A. Palano[21] , M. Palutan[25] , G. Panshin[41] , L. Paolucci[54] ,
A. Papanestis[55] , M. Pappagallo[21,h] , L.L. Pappalardo[23,k] , C. Pappenheimer[63] ,
C. Parkes[60,46] , B. Passalacqua[23,k] , G. Passaleva[24] , D. Passaro[32,r] , A. Pastore[21] ,
M. Patel[59] , J. Patoc[61] , C. Patrignani[22,i] , C.J. Pawley[76] , A. Pellegrino[35] ,

M. Pepe Altarelli[25], S. Perazzini[22], D. Pereima[41], A. Pereiro Castro[44], P. Perret[11],
A. Perro[46], K. Petridis[52], A. Petrolini[26,m], S. Petrucci[56], H. Pham[66], L. Pica[32,r],
M. Piccini[31], B. Pietrzyk[10], G. Pietrzyk[13], D. Pinci[33], F. Pisani[46],
M. Pizzichemi[28,o], V. Placinta[40], M. Plo Casasus[44], F. Polci[15,46], M. Poli Lener[25],
A. Poluektov[12], N. Polukhina[41], I. Polyakov[46], E. Polycarpo[3], S. Ponce[46],
D. Popov[7], S. Poslavskii[41], K. Prasanth[38], L. Promberger[19], C. Prouve[44],
V. Pugatch[50], V. Puill[13], G. Punzi[32,s], H.R. Qi[4], W. Qian[7], N. Qin[4], S. Qu[4],
R. Quagliani[47], B. Rachwal[37], J.H. Rademacker[52], M. Rama[32], M.
Ramírez García[79], M. Ramos Pernas[54], M.S. Rangel[3], F. Ratnikov[41], G. Raven[36],
M. Rebollo De Miguel[45], F. Redi[46], J. Reich[52], F. Reiss[60], Z. Ren[4],
P.K. Resmi[61], R. Ribatti[32,r], G. R. Ricart[14,80], D. Riccardi[32,r], S. Ricciardi[55],
K. Richardson[62], M. Richardson-Slipper[56], K. Rinnert[58], P. Robbe[13],
G. Robertson[56], E. Rodrigues[58,46], E. Rodriguez Fernandez[44],
J.A. Rodriguez Lopez[72], E. Rodriguez Rodriguez[44], A. Rogovskiy[55], D.L. Rolf[46],
A. Rollings[61], P. Roloff[46], V. Romanovskiy[41], M. Romero Lamas[44],
A. Romero Vidal[44], G. Romolini[23], F. Ronchetti[47], M. Rotondo[25], S. R. Roy[19],
M.S. Rudolph[66], T. Ruf[46], R.A. Ruiz Fernandez[44], J. Ruiz Vidal[78,z],
A. Ryzhikov[41], J. Ryzka[37], J.J. Saborido Silva[44], R. Sadek[14], N. Sagidova[41],
N. Sahoo[51], B. Saitta[29,j], M. Salomoni[46], C. Sanchez Gras[35], I. Sanderswood[45],
R. Santacesaria[33], C. Santamarina Rios[44], M. Santimaria[25], L. Santoro [2],
E. Santovetti[34], D. Saranin[41], G. Sarpis[56], M. Sarpis[73], A. Sarti[33],
C. Satriano[33,t], A. Satta[34], M. Saur[6], D. Savrina[41], H. Sazak[11],
L.G. Scantlebury Smead[61], A. Scarabotto[15], S. Schael[16], S. Scherl[58], A. M.
Schertz[74], M. Schiller[57], H. Schindler[46], M. Schmelling[18], B. Schmidt[46],
S. Schmitt[16], H. Schmitz[73], O. Schneider[47], A. Schopper[46], N. Schulte[17],
S. Schulte[47], M.H. Schune[13], R. Schwemmer[46], G. Schwering[16], B. Sciascia[25],
A. Sciuccati[46], S. Sellam[44], A. Semennikov[41], M. Senghi Soares[36], A. Sergi[26,m],
N. Serra[48,46], L. Sestini[30], A. Seuthe[17], Y. Shang[6], D.M. Shangase[79],
M. Shapkin[41], I. Shchemerov[41], L. Shchutska[47], T. Shears[58], L. Shekhtman[41],
Z. Shen[6], S. Sheng[5,7], V. Shevchenko[41], B. Shi[7], E.B. Shields[28,o], Y. Shimizu[13],
E. Shmanin[41], R. Shorkin[41], J.D. Shupperd[66], R. Silva Coutinho[66], G. Simi[30],
S. Simone[21,h], M. Singla[1], N. Skidmore[60], R. Skuza[19], T. Skwarnicki[66],
M.W. Slater[51], J.C. Smallwood[61], J.G. Smeaton[53], E. Smith[62], K. Smith[65],
M. Smith[59], A. Snoch[35], L. Soares Lavra[56], M.D. Sokoloff[63], F.J.P. Soler[57],
A. Solomin[41,52], A. Solovev[41], I. Solovyev[41], R. Song[1], Y. Song[47], Y. Song[4], Y. S.
Song[6], F.L. Souza De Almeida[3], B. Souza De Paula[3], E. Spadaro Norella[27,n],
E. Spedicato[22], J.G. Speer[17], E. Spiridenkov[41], P. Spradlin[57], V. Sriskaran[46],
F. Stagni[46], M. Stahl[46], S. Stahl[46], S. Stanislaus[61], E.N. Stein[46], O. Steinkamp[48],
O. Stenyakin[41], H. Stevens[17], D. Strekalina[41], Y. Su[7], F. Suljik[61], J. Sun[29],
L. Sun[71], Y. Sun[64], P.N. Swallow[51], K. Swientek[37], F. Swystun[54], A. Szabelski[39],
T. Szumlak[37], M. Szymanski[46], Y. Tan[4], S. Taneja[60], M.D. Tat[61], A. Terentev[48],
F. Terzuoli[32,v], F. Teubert[46], E. Thomas[46], D.J.D. Thompson[51], H. Tilquin[59],
V. Tisserand[11], S. T'Jampens[10], M. Tobin[5], L. Tomassetti[23,k], G. Tonani[27,n],
X. Tong[6], D. Torres Machado[2], L. Toscano[17], D.Y. Tou[4], C. Trippl[42], G. Tuci[19],
N. Tuning[35], L.H. Uecker[19], A. Ukleja[37], D.J. Unverzagt[19], E. Ursov[41],
A. Usachov[36], A. Ustyuzhanin[41], U. Uwer[19], V. Vagnoni[22], A. Valassi[46],
G. Valenti[22], N. Valls Canudas[42], M. Van Dijk[47], H. Van Hecke[65],
E. van Herwijnen[59], C.B. Van Hulse[44,x], R. Van Laak[47], M. van Veghel[35],
R. Vazquez Gomez[43], P. Vazquez Regueiro[44], C. Vázquez Sierra[44], S. Vecchi[23],
J.J. Velthuis[52], M. Veltri[24,w], A. Venkateswaran[47], M. Vesterinen[54], D. Vieira[63],

M. Vieites Diaz[46] , X. Vilasis-Cardona[42] , E. Vilella Figueras[58] , A. Villa[22] ,
P. Vincent[15] , F.C. Volle[13] , D. vom Bruch[12] , V. Vorobyev[41], N. Voropaev[41] ,
K. Vos[76] , C. Vrahas[56] , J. Walsh[32] , E.J. Walton[1] , G. Wan[6] , C. Wang[19] ,
G. Wang[8] , J. Wang[6] , J. Wang[5] , J. Wang[4] , J. Wang[71] , M. Wang[27] , N. W.
Wang[7] , R. Wang[52] , X. Wang[69] , Y. Wang[8] , Z. Wang[13] , Z. Wang[4] , Z. Wang[7] ,
J.A. Ward[54,1] , N.K. Watson[51] , D. Websdale[59] , Y. Wei[6] , B.D.C. Westhenry[52] ,
D.J. White[60] , M. Whitehead[57] , A.R. Wiederhold[54] , D. Wiedner[17] , G. Wilkinson[61] ,
M.K. Wilkinson[63] , M. Williams[62] , M.R.J. Williams[56] , R. Williams[53] ,
F.F. Wilson[55] , W. Wislicki[39] , M. Witek[38] , L. Witola[19] , C.P. Wong[65] ,
G. Wormser[13] , S.A. Wotton[53] , H. Wu[66] , J. Wu[8] , Y. Wu[6] , K. Wyllie[46] , S. Xian[69],
Z. Xiang[5] , Y. Xie[8] , A. Xu[32] , J. Xu[7] , L. Xu[4] , L. Xu[4] , M. Xu[54] , Z. Xu[11] ,
Z. Xu[7] , Z. Xu[5] , D. Yang[4] , S. Yang[7] , X. Yang[6] , Y. Yang[26,m] , Z. Yang[6] ,
Z. Yang[64] , V. Yeroshenko[13] , H. Yeung[60] , H. Yin[8] , C. Y. Yu[6] , J. Yu[68] ,
X. Yuan[5] , E. Zaffaroni[47] , M. Zavertyaev[18] , M. Zdybal[38] , M. Zeng[4] , C. Zhang[6] ,
D. Zhang[8] , J. Zhang[7] , L. Zhang[4] , S. Zhang[68] , S. Zhang[6] , Y. Zhang[6] , Y. Zhang[61],
Y. Z. Zhang[4] , Y. Zhao[19] , A. Zharkova[41] , A. Zhelezov[19] , X. Z. Zheng[4] ,
Y. Zheng[7] , T. Zhou[6] , X. Zhou[8] , Y. Zhou[7] , V. Zhovkovska[13] , L. Z. Zhu[7] ,
X. Zhu[4] , X. Zhu[8] , Z. Zhu[7] , V. Zhukov[16,41] , J. Zhuo[45] , Q. Zou[5,7] ,
S. Zucchelli[22,i] , D. Zuliani[30] , G. Zunica[60] .

[1] School of Physics and Astronomy, Monash University, Melbourne, Australia
[2] Centro Brasileiro de Pesquisas Físicas (CBPF), Rio de Janeiro, Brazil
[3] Universidade Federal do Rio de Janeiro (UFRJ), Rio de Janeiro, Brazil
[4] Center for High Energy Physics, Tsinghua University, Beijing, China
[5] Institute Of High Energy Physics (IHEP), Beijing, China
[6] School of Physics State Key Laboratory of Nuclear Physics and Technology, Peking University, Beijing, China
[7] University of Chinese Academy of Sciences, Beijing, China
[8] Institute of Particle Physics, Central China Normal University, Wuhan, Hubei, China
[9] Consejo Nacional de Rectores (CONARE), San Jose, Costa Rica
[10] Université Savoie Mont Blanc, CNRS, IN2P3-LAPP, Annecy, France
[11] Université Clermont Auvergne, CNRS/IN2P3, LPC, Clermont-Ferrand, France
[12] Aix Marseille Univ, CNRS/IN2P3, CPPM, Marseille, France
[13] Université Paris-Saclay, CNRS/IN2P3, IJCLab, Orsay, France
[14] Laboratoire Leprince-Ringuet, CNRS/IN2P3, Ecole Polytechnique, Institut Polytechnique de Paris, Palaiseau, France
[15] LPNHE, Sorbonne Université, Paris Diderot Sorbonne Paris Cité, CNRS/IN2P3, Paris, France
[16] I. Physikalisches Institut, RWTH Aachen University, Aachen, Germany
[17] Fakultät Physik, Technische Universität Dortmund, Dortmund, Germany
[18] Max-Planck-Institut für Kernphysik (MPIK), Heidelberg, Germany
[19] Physikalisches Institut, Ruprecht-Karls-Universität Heidelberg, Heidelberg, Germany
[20] School of Physics, University College Dublin, Dublin, Ireland
[21] INFN Sezione di Bari, Bari, Italy
[22] INFN Sezione di Bologna, Bologna, Italy
[23] INFN Sezione di Ferrara, Ferrara, Italy
[24] INFN Sezione di Firenze, Firenze, Italy
[25] INFN Laboratori Nazionali di Frascati, Frascati, Italy
[26] INFN Sezione di Genova, Genova, Italy
[27] INFN Sezione di Milano, Milano, Italy
[28] INFN Sezione di Milano-Bicocca, Milano, Italy
[29] INFN Sezione di Cagliari, Monserrato, Italy
[30] Università degli Studi di Padova, Università e INFN, Padova, Padova, Italy
[31] INFN Sezione di Perugia, Perugia, Italy
[32] INFN Sezione di Pisa, Pisa, Italy

[33] INFN Sezione di Roma La Sapienza, Roma, Italy

[34] INFN Sezione di Roma Tor Vergata, Roma, Italy

[35] Nikhef National Institute for Subatomic Physics, Amsterdam, Netherlands

[36] Nikhef National Institute for Subatomic Physics and VU University Amsterdam, Amsterdam, Netherlands

[37] AGH - University of Science and Technology, Faculty of Physics and Applied Computer Science, Kraków, Poland

[38] Henryk Niewodniczanski Institute of Nuclear Physics Polish Academy of Sciences, Kraków, Poland

[39] National Center for Nuclear Research (NCBJ), Warsaw, Poland

[40] Horia Hulubei National Institute of Physics and Nuclear Engineering, Bucharest-Magurele, Romania

[41] Affiliated with an institute covered by a cooperation agreement with CERN

[42] DS4DS, La Salle, Universitat Ramon Llull, Barcelona, Spain

[43] ICCUB, Universitat de Barcelona, Barcelona, Spain

[44] Instituto Galego de Física de Altas Enerxías (IGFAE), Universidade de Santiago de Compostela, Santiago de Compostela, Spain

[45] Instituto de Fisica Corpuscular, Centro Mixto Universidad de Valencia - CSIC, Valencia, Spain

[46] European Organization for Nuclear Research (CERN), Geneva, Switzerland

[47] Institute of Physics, Ecole Polytechnique Fédérale de Lausanne (EPFL), Lausanne, Switzerland

[48] Physik-Institut, Universität Zürich, Zürich, Switzerland

[49] NSC Kharkiv Institute of Physics and Technology (NSC KIPT), Kharkiv, Ukraine

[50] Institute for Nuclear Research of the National Academy of Sciences (KINR), Kyiv, Ukraine

[51] University of Birmingham, Birmingham, United Kingdom

[52] H.H. Wills Physics Laboratory, University of Bristol, Bristol, United Kingdom

[53] Cavendish Laboratory, University of Cambridge, Cambridge, United Kingdom

[54] Department of Physics, University of Warwick, Coventry, United Kingdom

[55] STFC Rutherford Appleton Laboratory, Didcot, United Kingdom

[56] School of Physics and Astronomy, University of Edinburgh, Edinburgh, United Kingdom

[57] School of Physics and Astronomy, University of Glasgow, Glasgow, United Kingdom

[58] Oliver Lodge Laboratory, University of Liverpool, Liverpool, United Kingdom

[59] Imperial College London, London, United Kingdom

[60] Department of Physics and Astronomy, University of Manchester, Manchester, United Kingdom

[61] Department of Physics, University of Oxford, Oxford, United Kingdom

[62] Massachusetts Institute of Technology, Cambridge, MA, United States

[63] University of Cincinnati, Cincinnati, OH, United States

[64] University of Maryland, College Park, MD, United States

[65] Los Alamos National Laboratory (LANL), Los Alamos, NM, United States

[66] Syracuse University, Syracuse, NY, United States

[67] Pontifícia Universidade Católica do Rio de Janeiro (PUC-Rio), Rio de Janeiro, Brazil, associated to [3]

[68] School of Physics and Electronics, Hunan University, Changsha City, China, associated to [8]

[69] Guangdong Provincial Key Laboratory of Nuclear Science, Guangdong-Hong Kong Joint Laboratory of Quantum Matter, Institute of Quantum Matter, South China Normal University, Guangzhou, China, associated to [4]

[70] Lanzhou University, Lanzhou, China, associated to [5]

[71] School of Physics and Technology, Wuhan University, Wuhan, China, associated to [4]

[72] Departamento de Fisica , Universidad Nacional de Colombia, Bogota, Colombia, associated to [15]

[73] Universität Bonn - Helmholtz-Institut für Strahlen und Kernphysik, Bonn, Germany, associated to [19]

[74] Eotvos Lorand University, Budapest, Hungary, associated to [46]

[75] Van Swinderen Institute, University of Groningen, Groningen, Netherlands, associated to [35]

[76] Universiteit Maastricht, Maastricht, Netherlands, associated to [35]

[77] Tadeusz Kosciuszko Cracow University of Technology, Cracow, Poland, associated to [38]

[78] Department of Physics and Astronomy, Uppsala University, Uppsala, Sweden, associated to [57]

[79] University of Michigan, Ann Arbor, MI, United States, associated to [66]

[80] Departement de Physique Nucleaire (SPhN), Gif-Sur-Yvette, France

[a] Universidade de Brasília, Brasília, Brazil

[b] Centro Federal de Educacão Tecnológica Celso Suckow da Fonseca, Rio De Janeiro, Brazil

[c] Central South U., Changsha, China

[d]Hangzhou Institute for Advanced Study, UCAS, Hangzhou, China

[e]LIP6, Sorbonne Universite, Paris, France

[f]Excellence Cluster ORIGINS, Munich, Germany

[g]Universidad Nacional Autónoma de Honduras, Tegucigalpa, Honduras

[h]Università di Bari, Bari, Italy

[i]Università di Bologna, Bologna, Italy

[j]Università di Cagliari, Cagliari, Italy

[k]Università di Ferrara, Ferrara, Italy

[l]Università di Firenze, Firenze, Italy

[m]Università di Genova, Genova, Italy

[n]Università degli Studi di Milano, Milano, Italy

[o]Università di Milano Bicocca, Milano, Italy

[p]Università di Padova, Padova, Italy

[q]Università di Perugia, Perugia, Italy

[r]Scuola Normale Superiore, Pisa, Italy

[s]Università di Pisa, Pisa, Italy

[t]Università della Basilicata, Potenza, Italy

[u]Università di Roma Tor Vergata, Roma, Italy

[v]Università di Siena, Siena, Italy

[w]Università di Urbino, Urbino, Italy

[x]Universidad de Alcalá, Alcalá de Henares , Spain

[y]Universidade da Coruña, Coruña, Spain

[z]Department of Physics/Division of Particle Physics, Lund, Sweden

[†]Deceased